The impact and significance of tephra deposition on a Holocene forest environment in the North Cascades, Washington, USA.

Joanne Egan[1, 2], William J. Fletcher[1], Tim E.H. Allott[1], Christine S. Lane[1], Jeff J. Blackford[3], Douglas H. Clark[4]

[1]Department of Geography, School of Environment, Education and Development, University of Manchester, Oxford Road, Manchester, M13 9PL, UK. Corresponding author email: joanne.egan@manchester.ac.uk, co-author email: will.fletcher@manchester.ac.uk, christine.lane@manchester.ac.uk, tim.allott@manchester.ac.uk.

[2]Department of Geography, Edge Hill University, St Helens Road, Ormskirk, Lancashire, L39 4QP, email: eganj@edgehill.ac.uk

[3]Department of Geography, Environment and Earth Science, University of Hull, Cottingham Road, Hull, HU6 7RX, UK, email: j.blackford@hull.ac.uk

[4]Geology Department, Western Washington University, Bellingham, Washington, 98225-9080, USA, email: Doug.Clark@wwu.edu

Abstract

High-resolution palaeoecological analyses (stratigraphy, tephra geochemistry, radiocarbon dating, pollen and ordination) were used to reconstruct a Holocene vegetation history of a watershed in the Pacific Northwest of America to evaluate the effects and duration of tephra deposition on a forest environment and the significance of these effects compared to long-term trends. Three tephra deposits were detected and evaluated: MLF-T158 and MLC-T324 from the climactic eruption of Mount Mazama, MLC-T480 from a Late Pleistocene eruption of Mount Mazama and MLC-T485 from a Glacier Peak eruption. Records were examined from both the centre and fringe of the basin to elucidate regional and local effects. The significance of tephra impacts independent of underlying long-term trends was confirmed using partial redundancy analysis. Tephra deposition from the climactic eruption of Mount Mazama approximately 7600 cal. years BP caused a significant local impact, reflected in the fringe location by changes to open habitat vegetation (Cyperaceae and Poaceae) and changes in aquatic macrophytes (*Myriophyllum spicatum*, *Potamogeton, Equisetum* and the alga *Pediastrum*). There was no significant impact of the climactic Mazama tephra or other tephras detected on the pollen record of the central core. Changes in this core are potentially climate driven. Overall, significant tephra fall was demonstrated through high resolution analyses indicating a local effect on the terrestrial and aquatic environment, but there was no significant impact on the regional forest dependent of underlying environmental changes.

Key words: Tephra impact; Holocene environmental change; Pollen; Mazama; Glacier Peak; Redundancy analysis.

1. Introduction

Volcanic events can impact forest dynamics through a variety of mechanisms and at a variety of spatial scales. These impacts include high-severity, rapid plant mortality, particularly within the blast zone or in areas adjacent (proximal) to the eruption, but can also include impacts at wider (distal) spatial scales caused by either the direct effects of ash (tephra) deposition (Antos and Zobel, 2005) or by acidic or heavy metal deposition associated with volcanic eruptions (Blackford et al. 1992; Hotes et al. 2001).

Volcanic eruptions release gases into the atmosphere including CO_2, SO_2, HCl and HF (Delmelle et al. 2002) that may be deposited as acidic precipitation, dry deposition, acidic aerosols or by adhering to tephra particles (Delmelle et al. 2001). Impacts on vegetation from such acids range from lesions and burnt spots to total defoliation and death (Delmelle et al. 2002). Elements such as Cl, S, Na, Ca, K, Si, and Mg may be released both on contact with water and through leaching (Hotes et al. 2004) and may supply nutrients which can be limiting in an oligotrophic ecosystem (such as K) or toxic to some organisms (such as Zn, Cu, Cd, Pb and Ba) and inhibit biological growth both in terrestrial and aquatic ecosystems

(Chakraborty et al. 2010; Martin et al. 2009). Conversely, some elements can encourage biological growth by improving the productivity of the soils with the formation of non-crystalline materials (i.e. Al/Fe-humus complexes) and the accumulation of organic carbon, the two dominant pedogenic processes occurring in volcanic soils (Ugolini and Dahlgren, 2002).

The direct effects of tephra deposition include the abrasion of plant surfaces (reducing flowering) (Black and Mack, 1984), reductions in photosynthesis (Cook et al. 1981), blocking of stomata, which impede gas exchange between soil and atmosphere (Hinckley et al. 1984), and crushing of plant tissues (Antos and Zobel, 1985; Grishin et al. 1996) which reduces the general health of plants and can contribute to a structural change in the community. Tephra deposition can also result in high turbidity in the littoral zone of aquatic ecosystems (Lallement et al. 2016), reducing light penetration and impacting on photosynthetic activity.

The ash component of tephra has a wide variety of sizes that decrease with distance from the volcano. Particle diameters can range from 'very fine' (<30 μm), 'fine' (between 30 and 100 μm), 'coarse' (between 100 and 2,000 μm) and 'very coarse' (>2,000 μm) (Rose and Durant, 2009). The 'fine' to 'very fine' classes are particularly importance as they have the longest atmospheric residence times, travel the furthest distance (distal tephra) and carry the most toxic volatiles, which makes them particularly hazardous to the environment (Rose and Durant, 2009). In addition, Payne and Blackford (2008) argue that in some environments, distal tephras could be associated with greater impacts than proximal layers due to the concentration of the volatiles, especially the aerosol H_2SO_4 that can be deposited.

Distal tephra deposition has been identified as a cause of significant change in forest vegetation (Antos and Zobel, 2005; Hotes et al. 2006; Millar et al. 2006) with long lasting impacts associated with volcanic eruptions, evidenced for example by the environmental impacts of the 1980 eruption of Mount St. Helens that have persisted for over 35 years (Frenzen, 2000; Zobel and Antos, 1997). Studies of contemporary volcanic events have therefore been important in demonstrating ecosystem impacts, but are limited both in their number, in the scale of events that can be evaluated, and in their ability to study long-term (decadal) forest trends following volcanic impacts (Hotes et al. 2004; Payne and Blackford, 2005).

Conversely, palaeo-environmental records have been used to infer longer-term volcanic impacts including the persistence of associated vegetation change and trajectories of recovery. Several workers have demonstrated long-term community scale change at geographically distal locations from the eruption source. For example, Blackford et al. (1992) reported a decline in *Pinus sylvestris* attributed to acid loading from the deposition of tephra from Hekla 4 (Blackford et al. 1992). Studies of the deposition of tephra from Aniakchak II (Blackford et al. 2014) and Laacher See (Birks and Lotter, 1994) showed shifts from Cyperaceae-dominated assemblages to Poaceae-dominated vegetation cover, suggesting a shift to drier and/or more nutrient-rich ecosystems. In New Zealand Giles et al. (1999) showed increases in degraded pollen following tephra deposition from Kaharoa with the temporary extinction of *Leucopogon fasciculatus* and *Tupeia antarctica* attributed to acid loading or mechanical damage due to the tephra, and a particularly notable increase in *Leptospermum* pollen due to the opening of the canopy. However other studies have reported no impacts on vegetation associated with distal tephra deposition (Caseldine et al. 1998; Hall et al. 1994; Hall, 2003; Lotter and Birks, 1993).

The detection and type of responses in both present day and palaeo-investigations can vary due to several important factors such as: the tephra layer thickness (Thorarinsson, 1979), distance from the source (Grishin et al. 1996; Millar et al. 2006), the type and sensitivity of the receiving environment (Hotes et al. 2006), the vulnerability and sensitivity of specific vegetation types (Antos and Zobel, 1985, 2005; Zobel and Antos, 1997), and ongoing environmental change in that specific location (Blackford et al. 2014). The temporal resolution of the study is also important because effects may last for millennia (Kilian et al. 2006) or only a few decades (Giles et al. 1999), and these decadal effects can be missed if the stratigraphic sampling resolution is low.

This study focuses on the distal impacts of 'fine' to 'very fine' ash as there is much less known about the distal impacts compared to the proximal impacts of tephra deposition (Telford et al. 2004: 2337). We present vegetation records from Moss Lake, Washington State (Figure 1) using detailed stratigraphic and geochronological analyses and high-resolution pollen analysis. The specific aims of the study are to (1) evaluate the impacts of distal tephra deposition events on forest vegetation and (2) assess the significance of the impacts in relation to longer-term Holocene environmental shifts (Figure 2).

During the Late Pleistocene and through the Holocene major tephra producing eruptions from Glacier Peak and Mount Mazama in the Cascade Range deposited tephra over much of the Pacific Northwest of America. Three plinian eruptions of Glacier Peak between 13,710-13,410 cal. years BP (2σ) (Kuehn et al. 2009) and 11,070-11,530 cal. years BP (2σ) (Porter, 1978) deposited tephra 500-1000 km^2 to the south and east of the volcano (Porter, 1978; Wood and Baldridge, 1990). The plinian eruption of Mount Mazama, at 7682-7584 cal. years BP (95.4% probability range) (Egan et al. 2015) ejected nearly 50 km^3 of rhyodacitic pumice into the atmosphere (ten times as much as the 1980 eruption of Mount St Helens), and deposited ash over an area of approximately $1.7x10^6$ km^2 (Zdanowicz et al. 1999) in a predominantly north-easterly direction (Figure 1).

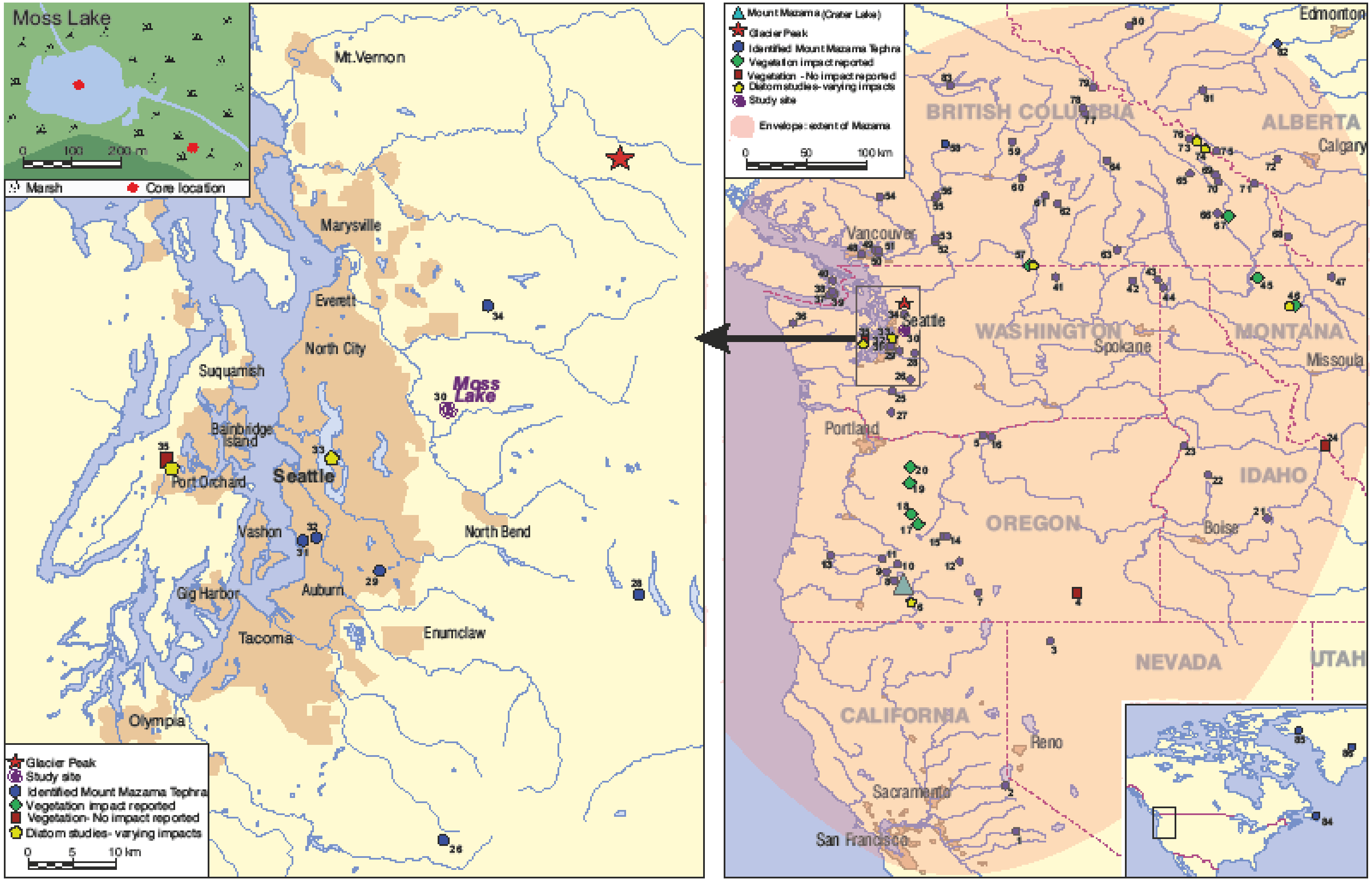

Figure 1: Extent of deposition from the Plinian eruption of Mount Mazama, and sites where it has previously been identified. The elliptical shaded envelope in the map to the right shows the extent of recorded visible Mount Mazama tephra deposition. True tephra dispersal was much

greater with cryptotephra having been found as far as Newfoundland (Pyne-O'Donnell et al. 2012) and Greenland (Zdanowicz et al., 1999). The locations of Moss Lake, Mount Mazama and Glacier Peak are also highlighted. The shading around cities indicates the size and distribution of major urban areas. A key is provided for the numbered sites in supplementary materials (A, Table 1).

Considering the scale of tephra deposition from these eruptions there has been minimal examination of the impacts on terrestrial ecosystems. Glacier Peak tephra has been identified in Washington and northern Oregon, but there has only been one study that has concentrated on the impact of tephra deposition from this eruption reporting no impact (Blinman et al. 1979). Despite the large number of studies that have identified Mazama tephra in stratigraphic deposits throughout the Pacific Northwest and as far east as Newfoundland (Figure 1) only ten studies have considered the terrestrial effects of the eruption and subsequent widespread tephra deposition. These studies reported impacts including vegetation compositional change (Blinman et al. 1979; Heinrichs et al. 1999; Long et al. 2011; Mack et al. 1978; Mack et al. 1983; Mehringer et al. 1977a), reduced pollen productivity (Power et al. 2011), wildfire suppression (Power et al. 2011), wildfire enhancement (Beierle and Smith, 1998; Long et al. 2014), and nutrient changes affecting lake algae (Blinman et al. 1979). Two of the ten studies reported no impacts (e.g. Blinman et al. 1979 (Wildcat Lake, Wildhorse Lake); Mehringer et al. 1977b (Loss Trail Pass bog)).

These studies clearly illustrate the ambiguity of the effects of tephra deposition on terrestrial ecosystems with varying, and some contradictory impacts. More studies are required for coherence. Previous studies assessing the impact of the Mazama tephra have tended to produce data from fairly coarse resolutions such as 2 cm^3 samples continuously along the cores (Blinman et al. 1979; Mehringer et al. 1977b), 1 cm^3 samples at 10 cm intervals (Mack et al. 1983) and continuous samples of 1 cm^3 (Mehringer et al. 1977a). Tephra impacts can last as little as a few decades (Giles et al. 1999) thus this study uses high resolution analyses aiming to achieve a decadal, or even sub-decadal resolution so there is little possibility that the impact is missed; a possibility in previous studies. Further, this study presents a quantitative analysis of the significance of vegetation changes associated with tephra deposition independent of underlying environmental trends, which has not been done for the impacts of Mazama before.

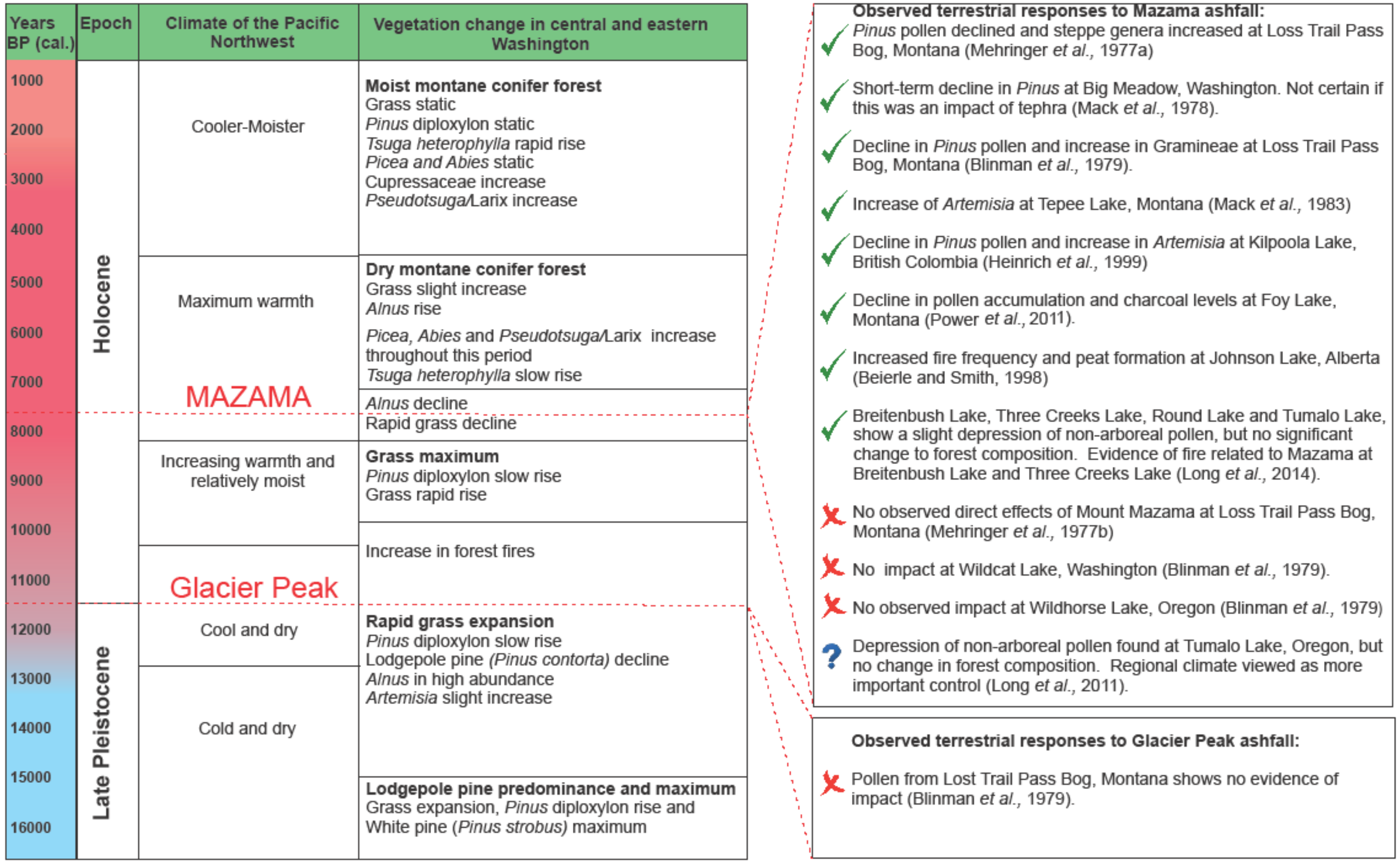

Figure 2: Climate and vegetation record of the Pacific Northwest and central/eastern Washington adapted from Hansen (1947), Whitlock (1992) Pritchard et al., (2009), Mustaphi et al., (2014). The text boxes to right summarise the main findings from previous studies about the impact of Mazama tephra and Glacier Peak tephra. The ticks represent those that observe an impact, and the crosses represent those that do not. These studies are subjective and qualitative and have not performed any statistics to test for impact significance.

2. Regional setting

Prior studies indicate that the climactic eruption of Mount Mazama was a high magnitude event producing the most significant tephra fall of the Holocene in North America. The Mazama tephra is of great stratigraphic importance and has been identified at Moss Lake. Moss Lake (N 47º 41’ 35.7” W 121º 50’ 48.6”) is 500 km northeast of Crater Lake (the site of the Mazama eruptions) allowing distal impacts to be assessed, and 69 km south of Glacier Peak. There have been several Mazama tephra deposits found in close proximity (<50 km) to Moss Lake (e.g. Bear Swamp (Blackford, Pers. Comm); Swamp Lake (Blackford pers comm; Egan, Unpublished), Covington (Broecker et al. 1956), Bow Lake (Rubin and Alexander, 1960), Arrow Lake (Rubin and Alexander, 1960), Lake Washington (Abella, 1988; Leopold et al. 1982), Skykomish River (Tabor et al. 1963) and Wildcat Lake (Blinman et al. 1979)). Out of these only one has assessed the terrestrial impact of tephra deposition Wildcat Lake (Blinman et al. 1979), where a 25 mm deposit was reported to cause no impact. This study will thus add to current knowledge of the impacts of thin (<100 mm) tephra deposits composed of the ‘fine’ to ‘very fine’ size class west of the Cascade Range.

Moss Lake has a diameter of approximately 200 m with a maximum water depth of 4.5 m. Moss Lake occupies a shallow basin within a broad fluted basal till plain deposited during the Vashon Stade (~18,000-16,500 cal. years BP at the site; Porter and Swanson, 1998). This till sheet overlies glaciomarine drift and outwash deposits (Dragovich et al. 2002).

This area has a mild, maritime climate with a mean annual temperature of 8-10 °C, and mean annual precipitation total of 1500-2500 mm with winter seeing about 90% of the annual accumulation (NOAA, 2014). The dominant vegetation in this area is a mix of forest trees: Douglas Fir (*Pseudotsuga menziesii*), Western Red Cedar (*Thuja plicata*), Silver Fir (*Abies* *amabilis*), Western Hemlock (*Tsuga heterophylla*), Lodgepole Pine (*Pinus contorta*), Western White Pine (*Pinus monitcola*), Western Larch (*Larix occidentalis*), Englemann Spruce (*Picea engelmannii*), Quaking Aspen (*Populus tremuloides*), Red Alder (*Alnus rubra*) and Sitka Alder (*Alnus sinuata*) (Brockman, 1968).

3. Material and methods

3.1. Core collection

Following classical palynological theory on site-source relationships (Jacobson and Bradshaw, 1981; Prentice, 1985), as the lake is 200 m in diameter there will be differing proportions of local, extra-local and regional pollen represented, with local pollen well represented at the lake fringe and regional pollen better represented at the lake centre. To allow an elucidation of local versus extra-local/regional signals two cores were collected from Moss Lake, one from the centre of the lake basin (MLC) and one at the wetland fringe of the lake adjacent to the contemporary forest vegetation (MLF).

MLC was collected from the deepest (water depth) point of Moss lake of 4.5 m, determined with an echo sounder, using a modified Livingstone corer. The core drive started at the sediment surface but the first 2 m were not sampled. Core retrieval began at 2 m and continued to a depth of 6 m at which point coring could not proceed further because of gravelly clays. Three visible tephra layers were observed in the core sequence at 485 cm, 480 cm and 324 cm of 10 mm, 10 mm and 40 mm thickness respectively. MLF was extracted from the fringe of Moss Lake using a Russian corer, reaching a depth of 2.5 m and bottoming clay sediments. The Mazama tephra was tentatively identified in MLF by its distinct orange/pale brown colour commonly observed (Mullineaux, 1974) brought about by weathering (Jones and Gislason, 2008). The cores were extruded into plastic guttering, wrapped in cling film and stored in the cold room (2-4°C) at The University of Manchester.

Data for MLC are presented from the complete stratigraphy retrieved, whereas pollen data from MLF is restricted to the stratigraphy immediately above and below the Mazama layer. This sampling design was used for MLF due to the relatively short core length (2.5 m) indicating a low-resolution Holocene record.

3.2.Stratigraphic analyses

A dual strategy was used for analysis of LOI and carbonate content. Contiguous 10 mm samples were taken throughout the core sequences of both MLC and MLF. Additionally, samples at 5 mm resolution were taken in the core sections encompassing 30 mm below to 30 mm above each identified tephra layer, with 5 mm sampling resolution also employed within each tephra layer. Standard ashing procedures were employed, heating the samples at 550 ^{o}C for the organic content and 925^{o}C for the carbonate content (Veres, 2002). LOI is used partially as an indicator of the changing importance allochthonous inputs to the lake. Carbonate analysis is used to identify if there is likely to be a hard water effect for radiocarbon dating (Philippsen, 2013). Magnetic susceptibility for both cores was measured at low frequency (0.47 kHz) at room temperature using the loop scanner of a Bartington Instruments Ltd MS2 meter to help identify allocththonous, clastic inputs such as tephra. The loop sensor was stationary and the core was pushed through to take measurements every 10 mm down the core, taking a measurement for 10 seconds for each 10 mm section (Dearing, 1994). Particle size analysis was conducted in order to assist with the determination of the tephra layer boundary in MLF as it was not distinct. Samples were taken every 10 mm, and every 5 mm through the tephra layer, digested in hydrogen peroxide to remove the organics, and measured using a Malvern Mastersizer 2000.

3.3.Tephra geochemistry

Tephra glass shard compositions were analysed to identify the origin of the tephra layers by comparison with published data from regional tephra layers. Visible tephra samples at depths 485 cm, 4180cm and 324 cm in MLC and at 158 cm in MLF were wet-sieved at 25 µm to remove clays and fine silt particles. Samples were dried and mounted in epoxy resin before grinding and polishing to reveal cross sections of the glass shards suitable for geochemical analysis (Hunt and Hill 1993). Electron probe microanalysis using wavelength dispersive spectroscopy (WDS-EPMA) was used to measure major and minor element compositions of the tephra to confirm the source. All analyses were made on the JEOL-JXA8600 electron microprobe at the Research Laboratory for Archaeology and the History of Art, University of Oxford. An accelerating voltage of 15 keV, a 6 nA beam current, and a 10 µm defocussed beam spot were used. Peak counting times used were 10 seconds for Na; 30 seconds for Si, Al, Mg, K, Ca, Ti and Fe; 40 seconds for Mn; 50 seconds for Cl, and 60 seconds for P. Secondary standard glasses were analysed intermittently to monitor the instrument precision and accuracy (Jochum and Nohl, 2008). Secondary standard file summaries for each analysis session are in supplementary materials (B, Table 1): Max-Planck-Institut für Chemie, Germany (MPI-DING) fused volcanic glass standards ATHO-G (rhyolite), StHS6/80-G (andesite) and GOR132-G (Komatiite) were used (Jochum and Nohl, 2008). Tephra particle morphologies and approximate glass shard sizes were described following observations under a high-power petrographic light microscope.

3.4.Radiocarbon dating

Accelerator mass spectrometry (AMS) radiocarbon dating of eight bulk organic lake sediment samples from MLC and three bulk sediment samples from MLF was carried out. Bulk sediment was used as there were no identifiable macrofossils or macrocharcoal fragments suitable for dating in the sediment cores, even in MLF where sediments contained unidentifiable fragments less than 250 µm. The low carbonate content (see section 4.1.) and underlying geology indicates that hard water reservoir effects are unlikely, thus bulk samples are acceptable. Radiocarbon dates were calibrated to calendar years (cal. years BP) using OxCal v.4.2.4 (Bronk Ramsey, 2014) and the IntCal13 calibration curve (Reimer, 2013). An age-depth model was constructed through Bayesian modelling using a *P_sequence* deposition model in OxCal v.4.2.4, which included an "event free depth scale" to account for the instantaneous deposition of the 40 mm thick Mazama tephra (Staff et al., 2011). Modelling could not be done for MLF due to an age reversal above the tephra layer (see sections 4.3. and 5.2.2).

3.5.Pollen analysis

For MLC 121 pollen samples were counted and 81 for MLF. For MLC the general sampling resolution was coarse with samples taken every 50 mm throughout the majority of the core. The age-depth model suggests these contiguous samples represent approximately 50-200 years of sediment accumulation, sufficient to disclose changes in vegetation associated with large scale environmental changes (Birks and Birks, 1980). The sampling resolution was increased around the tephra layers with contiguous 10 mm samples taken 150 mm either side of the Mazama tephra layer, and then 5 mm contiguous samples taken 30 mm above and below all tephra deposits to identify short-term changes. The age-depth model suggests these samples represent approximately 10-20 years. For MLF 1 mm contiguous samples were taken 40 mm above and 20 mm below the Mazama tephra deposit to maximise potential stratigraphic resolution. The high resolution sampling avoided areas of tephra penetration outside of the primary tephra layer.

Samples were prepared for pollen analysis as follows. A volume of 0.6 ml of each sample was prepared in seven steps following Moore et al. (1991): i) adding HCl, ii) sieving at 180 µm to ensure larger conifer pollen was included, iii) KOH digestion, iv) HF to remove silicates (Heusser and Stock, 1984), v) acetolysis, vi) alcohol dehydration, vii) and mounted in silicone oil. At least 300 terrestrial pollen grains were counted for each sample, except for six samples with very low pollen concentrations where counts of 100 were made (two samples within the Mazama tephra of MLF, four samples within basal clay sediments of MLC). *Lycopodium* was added and counted in each sample to allow determination of pollen and charcoal concentrations. Micro-charcoal was counted alongside the pollen and counts were converted to charcoal concentrations (particles per gDW). *Pinus* pollen was attributed to the Diploxylon-type, *Pinus contorta* (Lodgepole pine) based on its dominance in previous studies in the area (e.g. Long et al., 2014; Prichard et al., 2009) and present-day biogeography (Brockman, 1968). Further, the Haploxylon-type pollen was not found.

Pollen diagrams presented here show the percentages of total land pollen (i.e. excluding spores and aquatics). The summary diagram illustrates the categorisation of pollen habitat preference, specifically water preference. Pollen concentration diagrams are also provided in Supplementary Materials D and E. Pollen zonation was used not only to assist with qualitative analyses, but also as a quantitative tool, as the zones determined represent significant changes in the assemblage. To statistically determine significant changes for the assemblage around specific tephra layers, optimal splitting by information content was used (Bennett, 1996). The Optimal approach is more robust than binary splitting for determining significant zones within these samples because it starts afresh for each successive number of zones, so there is no hierarchy of zones. The number of significant zones was determined through the use of the Broken-Stick model (Bennett, 1996). Pollen diagrams and the zonation were created using Psimpoll v.4.27 (Bennett, 2007).

3.6. Ordination and associated significance tests

Ordination was used to test for significant changes in the pollen record following the deposition of tephra, evaluating the significance of the impact of each tephra relative to and independently from additional environmental variables chosen to account for underlying environmental trends. Six different pollen biostratigraphies were used in these analyses; Total pollen taxa (including aquatics and spores) (%), arboreal pollen only (%), non-arboreal pollen only (%), wetland taxa only (%), aquatic taxa only (%) and pollen concentration (all taxa). The total sums for wetland and aquatic pollen were very low (<100), so greater caution is needed in interpreting these datasets. CANOCO 5 (ter Braak and Šmilauer, 2012) was used for all ordinations and associated statistical tests. Detrended Correspondence Analysis (DCA) (Hill and Gauch, 1980) was used initially to estimate the gradient lengths (as standard deviation units) of the different biostratigraphic data sets. All datasets in the study have short gradients (<1.7 SD), and consequently linear ordination methods were employed (Leps and Šmilauer, 2014). Principal Component Analysis (PCA) (Orloci, 1966) was then used to describe the relationships between different pollen species and samples in order to indicate possible environmental gradients.

The influence of three environmental variables (tephra, LOI and depth) on the pollen data was evaluated using direct ordination. Observed changes in the pollen assemblages around the time of volcanic events may have been a response to tephra deposition. This effect is modelled as an exponential decay function through time (Barker et al., 2000; Birks and Lotter, 1994; Blackford et al., 2014; Lotter and Anderson, 2012; Lotter and Birks, 1993). Prior to deposition of tephra, the tephra explanatory variable was given a value of 0 indicating no tephra. At the time of tephra deposition, a value of 100 is used, meaning the sediment is 100% tephra. Above the tephra layer the value of the tephra explanatory variable was decreased exponentially $x^{-\alpha t}$, where α is the decay coefficient and t is sample time (*f*= depth) since tephra deposition. In order to reflect different recovery times three decay coefficients were tested: the first had a decay coefficient of 0.8 to reflect the longest recovery time of approximately 500 years, the second had a decay coefficient of 0.5 to reflect medium duration or recovery of approximately 200 years, with most recovery having happened within approximately 100 years, and the final one had a decay coefficient of 0.1 to reflect the shortest recovery time of approximately 80 years, with most recovery having happened within approximately 20 years. There was little difference in the results (Table 2, supplementary material C) so the decay coefficient of 0.5 was used in the analysis presented here (see also Payne and Blackford, 2012).

LOI was the second environmental variable used, representing the inflow of exogenic material into the lake basin and associated local environmental changes. LOI was corrected for tephra by interpolating values for the samples between, over and underlying levels containing tephra. The third environmental variable employed in the analysis was depth, as a surrogate for possible long-term underlying directional change in the vegetation assemblages during the period of tephra deposition, associated for example with climate change or succession processes.

Variance partitioning (Borcard et al. 1992) using redundancy analysis was used to determine how much of the variation in pollen data is explained by each environmental variable and to test the significance of the three environmental variables within all six pollen datasets. Variance partitioning models showing significant relationships with any one or more of the environmental variables were then selected for Partial Redundancy Analysis (RDA) (ter Braak and Prentice, 1988; Rao, 1964), a constrained form of PCA, in order to test the significance of each environmental variable independent from the other two co-variables. Significance tests were made by comparing eigenvalues for the first RDA axes of the different biostratigraphies with the results of 999 permutations of Monte Carlo tests. Log transformation and double centring of the samples and environmental variables were used to allow for the closed compositional disposition of the data. The statistical results presented are not strongly influenced by the data treatments, as similar results are obtained with different ash values and decay coefficients (see supplementary materials C, Table 2).

4. Results

4.1.Stratigraphic analyses

Core MLC comprises three major stratigraphic units, MLCs-1, MLCs-2, and MLCs-3 (Figure 3). The basal unit MLCs-1 (590 cm – 495 cm) consists of clays and gravels with low LOI and high magnetic susceptibility values. Carbonates are low throughout. Within the two gravel units there are faceted stones representing glacial sediments. Gyttja dominates MLCs-2 (495 cm – 355 cm) and LOI increases up to 60%. Magnetic susceptibility decreases and remains low. MLCs-3 (355 cm – 200 cm) consists of a shift in stratigraphy to silty gyttja, reflected by the decrease of LOI followed by the development of more organic peaty silts and a coinciding increase of LOI. There is a sandy layer present at 230 cm with a slight increase in magnetic susceptibility and corresponding decrease in LOI. Where there are visible tephra deposits at 485 cm (MLC-T485), 480 cm (MLC-T480) and 324 cm (MLC-T324) LOI percentages decrease, falling as low as 5%, and magnetic susceptibility increases, especially at the layer MLC-T324.

Figure 3: Lithology, % LOI, magnetic susceptibility and carbonate content of MLC. The dotted line represents a 10x exaggeration of magnetic susceptibility to clearly see the smaller peaks.

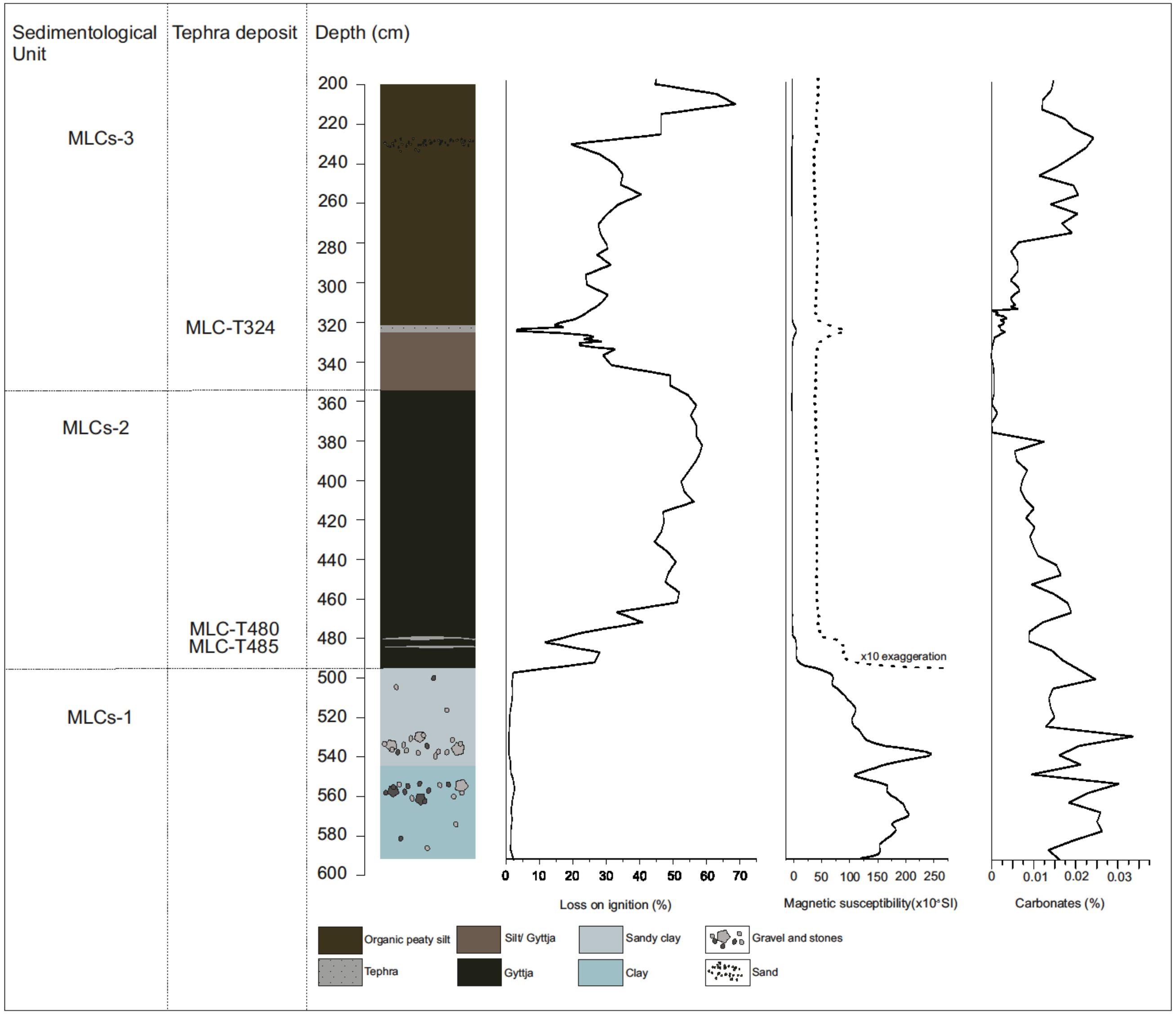

Figure 4 illustrates the stratigraphy, organic matter and carbonate content, magnetic susceptibility and particle size data for MLF. The core is primarily made up of sands and silts that gradually become more organic up core. MLFs-1 consists of organic sandy silts with low organic content and low magnetic susceptibility. Particle size analysis was used to determine the boundary of tephra deposition and shows a peak in coarse and fine sand between 158 and153 cm (MLF-T158), indicative of the tephra boundary with the coarse sand dominating the lower part of the tephra deposit reflecting the faster deposition or sinking of the heavier sediment. Within the tephra deposit LOI further decreases and magnetic susceptibility peaks. From 147 cm (MLFs-2) silty peats develop with an increasing LOI and generally low magnetic susceptibility. A silt unit is present from 146 to 132 cm. There is a brief increase of magnetic susceptibility and particle size at around 120 cm where there is a coarse sand deposit. Carbonate content is low throughout the core.

Figure 4: Lithology, % LOI, magnetic susceptibility, carbonate content and particle size of MLF

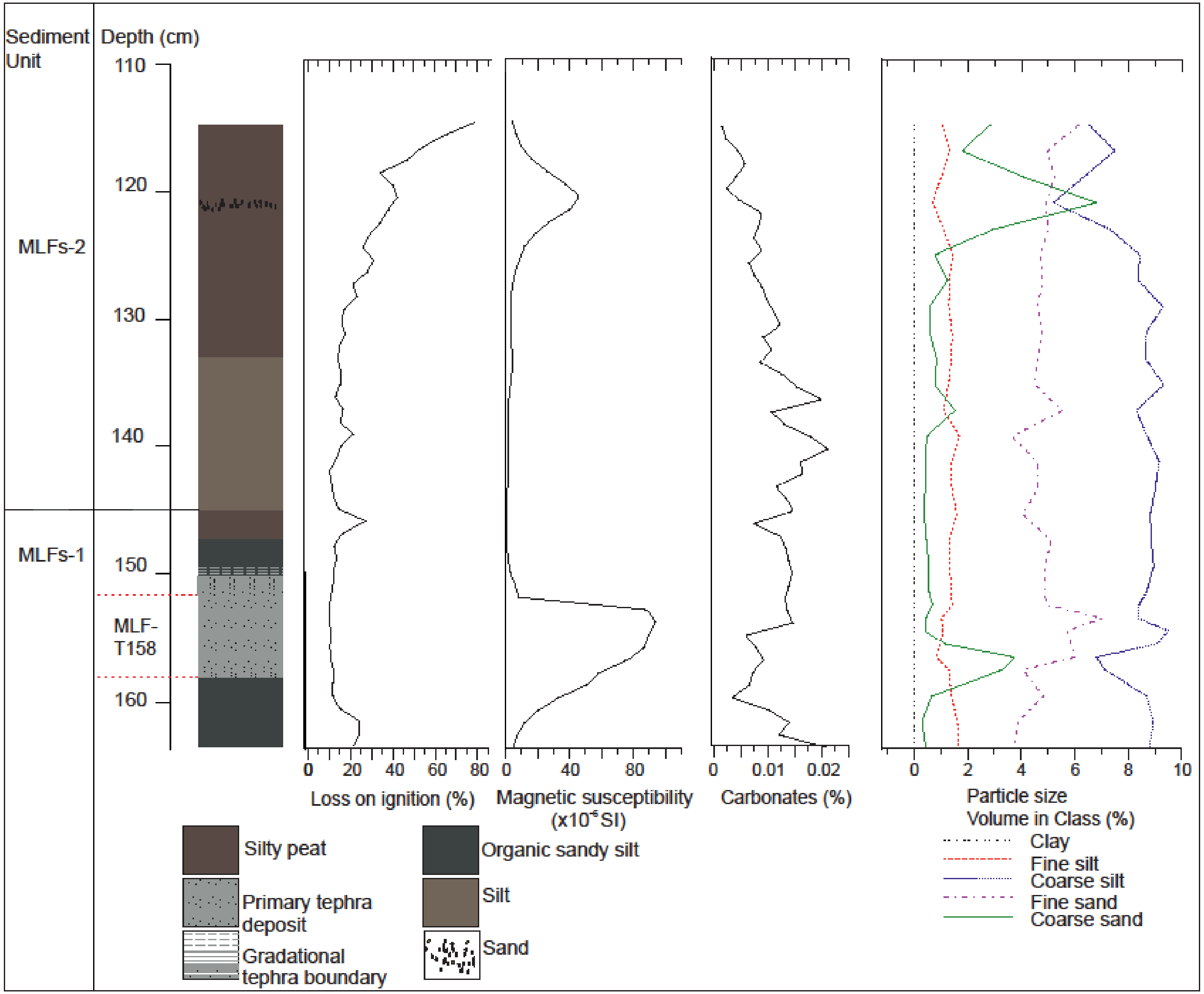

4.2. Tephra morphology and geochemistry

4.2.1. MLC-T324 morphology

The tephra layer MLC-T324 is 30 mm thick with clear, sharp boundaries and consists of grey "fine sand" sized (125 µm-250 µm) particles. Composed of more than 98% clear glass shards, MLC-T324 is characterised by angular, often platy, bubble-junction shards and vesicular to fluted shards that contain either closed or expanded elongate vesicles. Longest-axis lengths fall mainly within 60-180 µm, however larger shard sizes with longest axis lengths up to 320 µm are also present.

4.2.2. MLC-T480 morphology

MLC-T480 is composed of more than 98% clear glass shards. Morphologies range from bubble-junction shards with mostly expanded vesicles, to fluted shards with elongated vesicles. Shard longest axis lengths ranges are typically 40-120 µm, with rare shards having longest axis lengths of up to 180 µm.

4.2.3. MLC-T485 morphology

This represents the deepest tephra layer found in the core just before the transition to clay, MLC-T485 is approximately 7 mm thick with an almost identical appearance to MLC-T480. However, the glass shards from MLC-T485 have a distinctive morphology when compared to the other layers studied from Moss Lake. It is composed of approximately 80% glass shards, with the remainder of the sample plagioclase, prismatic pyroxene and hornblende minerals. The clear glass shards are highly vesicular, with variable closed, elongated and distorted vesicle forms. Shard morphologies are irregular and rather blocky, with sub-angular edges. Many shards contain microcrysts. Measurement of glass shard longest axis lengths show a dominant 60-160 µm range, with exceptional shards having longest axis lengths of up to 200 µm.

4.2.4. MLF-T158 morphology

MLF-T158 is approximately 50 mm thick but the boundaries are not well defined. The tephra is orange in colour and consists of coarse and fine sand-sized particles. The glass shards from MLF-T158 are identical in size and morphology to MLC-T324, however vesicular shards appear slightly yellow in colour. MLC-T480 is 8 mm thick and has the same colour and texture as MLC-T324 with well-defined boundaries.

4.2.5. Geochemistry

The geochemical results confirm that samples MLF-T158 and MLC-T324 are from the climactic eruption of Mount Mazama, which is illustrated well in Figure 5 (and Table 1) as the geochemical data are within the geochemical envelopes from reference samples. Geochemical analyses of MLC-T480 identify its source as an earlier Mazama eruption as the geochemistry shows a close similarity to reference data for Mazama (Figure 5). There are few if any records of this eruption; however, Bacon (1983) reconstructed Mount Mazama's eruptive history through geological mapping and reported an eruption approximately 12,000 years BP, it is likely that Maz-T480 is from this Late Pleistocene eruption supported by the radiocarbon dates and associated age-depth model presented here (Table 2). The third tephra layer MLC-T485 is geochemically attributed to Glacier Peak illustrated by the close geochemistry to the reference Glacier Peak tephras (Figure 5). Although difficult to distinguish the individual tephra layers from closely spaced eruptions of Glacier Peak between 13,710-11,070 cal. years BP based on geochemistry alone, the tephra is most similar to Glacier Peak G (13,710-13,410 cal. years BP at 2 sigma (Kuehn et al. 2009)) (Figure 5). However, due to the uncertainty and wide scatter of data points around the Glacier Peak ranges, we will refer to the layer as Glacier Peak (MLC-T485). The presence of microcrysts in these glass shards may explain some of the scatter within the glass geochemistry data (Figure 5) and the possibility of accidental probing of microcrysts.

Table 1: Major and minor element-oxide compositions for tephras found in Moss Lake. MLC-T324=Mazama (climactic eruption) in Moss Lake central, MLF-T158= Mazama (climactic eruption) in Moss Lake fringe, MLC-T480= Late Pleistocene Mazama, and MLC-T185= Glacier Peak tephra in Moss Lake central. Secondary standard file summaries for each analysis session are presented in supplementary materials (B, Table 1). Element oxide values presented are normalised to water-free values. Original analytical totals are shown. The summary reference data are the averages from the reference samples referred to in Figure 5.

	SiO_2	TiO_2	Al_2O_3	FeO	MnO	MgO	CaO	Na_2O	K_2O	P_2O_5	Cl_2O_3	Total
MLC-T485												
	77.70	0.18	12.48	0.94	0.00	0.11	0.98	3.50	3.90	0.04	0.16	95.04
	77.67	0.16	12.42	0.92	0.07	0.19	0.97	3.74	3.69	0.01	0.16	99.94
	78.02	0.16	12.43	0.95	0.01	0.18	0.92	3.53	3.66	0.03	0.14	99.30
	78.02	0.22	12.37	0.88	0.07	0.09	0.85	3.53	3.81	0.00	0.15	96.89
	78.12	0.20	12.16	0.89	0.01	0.14	0.81	3.61	3.90	0.00	0.15	95.16
	77.68	0.24	12.44	1.02	0.00	0.24	0.99	3.27	3.91	0.09	0.12	97.85
	77.59	0.17	12.48	1.00	0.03	0.21	0.93	3.70	3.72	0.04	0.12	98.96
	77.77	0.20	12.51	0.84	0.05	0.14	0.89	3.81	3.64	0.01	0.14	100.02
	77.93	0.16	12.31	0.92	0.00	0.15	0.89	3.68	3.75	0.06	0.13	99.06
	77.67	0.17	12.33	0.98	0.00	0.10	1.05	3.92	3.58	0.00	0.19	98.35
	78.15	0.23	12.42	0.79	0.06	0.14	1.02	3.31	3.67	0.05	0.16	95.84
	77.20	0.19	12.99	0.89	0.03	0.12	1.31	3.62	3.49	0.01	0.14	98.56
	77.41	0.24	12.16	1.06	0.05	0.20	0.95	3.94	3.74	0.06	0.18	96.16
MLC-T480												
	73.16	0.42	14.46	1.80	0.02	0.47	1.51	5.09	2.76	0.06	0.25	100.44
	73.29	0.46	14.33	1.95	0.11	0.45	1.59	4.80	2.72	0.03	0.27	99.13
	73.16	0.42	14.46	1.84	0.00	0.42	1.62	4.98	2.85	0.02	0.25	99.45
	72.98	0.44	14.45	1.74	0.11	0.43	1.63	5.09	2.82	0.07	0.23	99.40
	71.85	0.42	15.34	1.78	0.07	0.28	2.06	5.24	2.73	0.01	0.23	98.55
	73.17	0.44	14.40	1.84	0.07	0.45	1.57	4.94	2.78	0.10	0.24	99.70
	72.56	0.42	14.75	1.95	0.03	0.42	1.59	5.25	2.70	0.09	0.26	98.37
	72.86	0.43	14.57	1.91	0.11	0.45	1.61	4.96	2.86	0.05	0.19	98.64
	72.81	0.44	14.62	1.95	0.09	0.44	1.52	5.11	2.70	0.07	0.25	100.75
	73.12	0.41	14.49	1.85	0.09	0.37	1.59	4.94	2.75	0.13	0.26	97.71
MLC-T324												
	72.78	0.39	14.61	1.92	0.05	0.37	1.48	5.38	2.70	0.06	0.27	96.83
	73.04	0.46	14.31	1.90	0.02	0.48	1.51	5.37	2.58	0.08	0.26	98.56
	73.25	0.45	14.45	1.80	0.04	0.39	1.58	5.04	2.72	0.03	0.25	98.01
	72.95	0.45	14.61	1.91	0.02	0.42	1.58	4.93	2.82	0.05	0.26	97.49
	72.85	0.41	14.47	1.99	0.01	0.46	1.53	5.05	2.86	0.10	0.27	98.16
	73.16	0.39	14.24	1.95	0.01	0.42	1.61	5.23	2.60	0.11	0.27	98.30

	72.45	0.44	14.66	1.82	0.05	0.40	1.68	5.60	2.67	0.02	0.21	98.92
	73.23	0.37	14.38	1.86	0.11	0.44	1.61	4.85	2.80	0.07	0.29	95.12
	72.87	0.39	14.33	1.82	0.11	0.38	1.54	5.60	2.68	0.07	0.21	99.05
MLF-T158												
	72.68	0.44	14.53	1.98	0.09	0.40	1.55	5.31	2.73	0.03	0.26	100.50
	72.84	0.48	14.55	1.81	0.01	0.41	1.58	5.26	2.68	0.14	0.24	99.70
	72.79	0.43	14.53	1.82	0.00	0.48	1.58	5.40	2.69	0.03	0.25	99.48
	72.48	0.43	14.76	1.89	0.09	0.47	1.64	5.09	2.84	0.02	0.29	98.39
	72.92	0.45	14.60	1.87	0.04	0.48	1.62	5.03	2.68	0.03	0.29	98.33
	72.77	0.42	14.81	1.57	0.05	0.42	1.67	5.20	2.74	0.06	0.28	98.28
	71.33	0.38	15.52	1.66	0.08	0.39	2.25	5.74	2.31	0.10	0.23	97.83
	73.17	0.51	14.18	1.91	0.02	0.45	1.56	5.11	2.78	0.04	0.27	97.28
	73.40	0.43	14.14	1.91	0.09	0.46	1.45	5.00	2.76	0.08	0.28	97.12
	73.68	0.45	13.92	1.80	0.05	0.49	1.44	5.16	2.63	0.14	0.26	96.42
Mazama (Summary reference data)												
	71.23	0.40	14.03	1.88	0.06	0.42	1.53	5.01	2.67	-	0.18	
Glacier Peak (Summary reference data)												
	77.48	0.20	12.63	1.08	0.04	0.25	1.26	3.68	3.21	-	0.17	

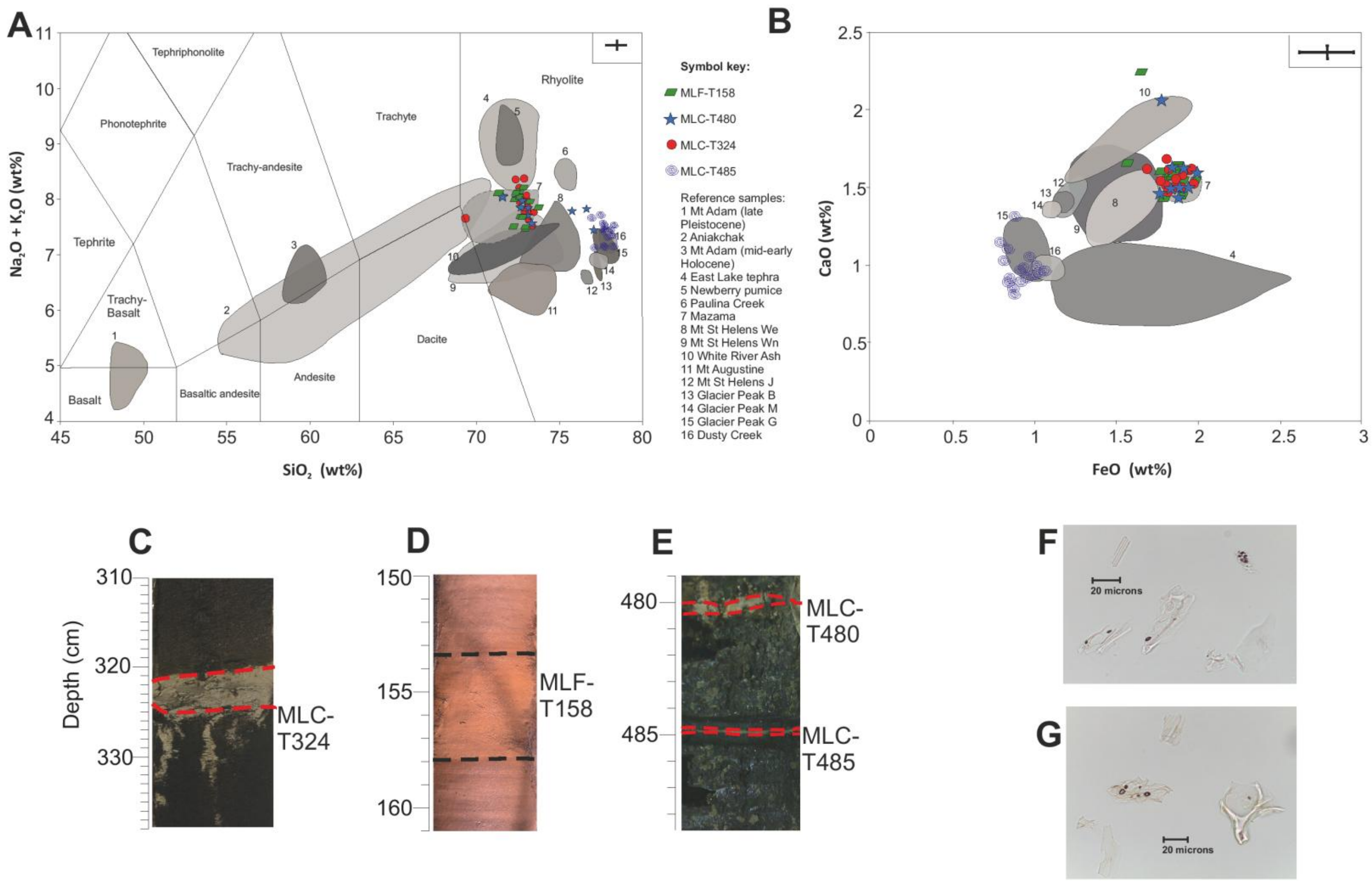

Figure 5: Plots (wt%) of selected element oxides from EPMA. (A) SiO_2/ Na_2O+K_2O bi-plot (B) FeO/CaO bi-plot. The different points reflect the different tephra units analysed in the core. The numbered ranges are the geochemical ranges of reference samples frequently found in this

region which are included for comparison (labelled 1-16). Reference samples 1 and 3 are from Hildreth and Fierstein (1997), 2, 4, 7, 8, 9, 10 and 11 from Pyne-O'Donnell et al., (2012), 5 and 6 are from (Kuehn and Foit, 2006), 13, 14 and 15 are from (Kuehn et al. 2009), and 12 and 16 are from (Hallett et al. 2001). The range for Mt. St. Helens is from combined geochemistry data as the compositions are similar. Data points have been normalised for data set comparison and outliers removed. The error bar at the top right of the bi-plots is to 2SD. (C) is the Mazama tephra layer from MLC (MLC-T324), (D) is the Mazama tephra layer from MLF (MLF-T158), (E) is the Glacier Peak (MLC-T485) and Late Pleistocene Mazama (MLC-T480) tephra layers from MLC, (F) are glass shards from MLC-T324 and (G) are glass shards from MLC-T158.

4.3. Radiocarbon dating

The MLC sediment record (excluding the clays) spans the late Pleistocene (16,294-12,789 cal. years BP (95.4% probability range)) to the late Holocene (2765-2307 cal. years BP (95.4% probability range)) (Table 2, Figure 6). It should be noted that the record does not capture recent sediment deposition because of the loss of sediment at the top during core collection. The model is well constrained within the Holocene, especially around the time of MLC-T324 (climactic Mazama) tephra deposition. There is more uncertainty around the ages in the late Pleistocene due to the low(er) density of available dating control points (one date) for this part of the model. Previous published ages for Glacier Peak tephra ranged from 13,710-13,410 cal. years BP (2σ) (Kuehn et al. 2009) and 11,070-11,530 cal. years BP (2σ) (Porter, 1978). These dates were not included in the model due to the uncertainty regarding the exact eruption the tephra represents. An attempt was made to include the previously published age ranges for Glacier Peak in the age-depth model but this actually compromised the accuracy of the model as larger errors were reported. The age-depth model provided here in Figure 6 suggests an overlapping age of 15,204-12,645 cal. years BP (95.4% probability range). The three radiocarbon dates for MLF demonstrated an age reversal in the top two samples and was confirmed by re-analysis of the samples (Table 2). The dates therefore cannot be used in the analyses, but are provided to demonstrate that MLF-T158 is within the right time period as the sediments below the tephra have a modelled age range of 7958-7795 cal. years BP (95.4% probability range). Therefore further up the core within the tephra layer the age is likely to be younger and within the previously published age range of 7682-7584 cal. years BP (95.4% probability range) (Egan et al. 2015).

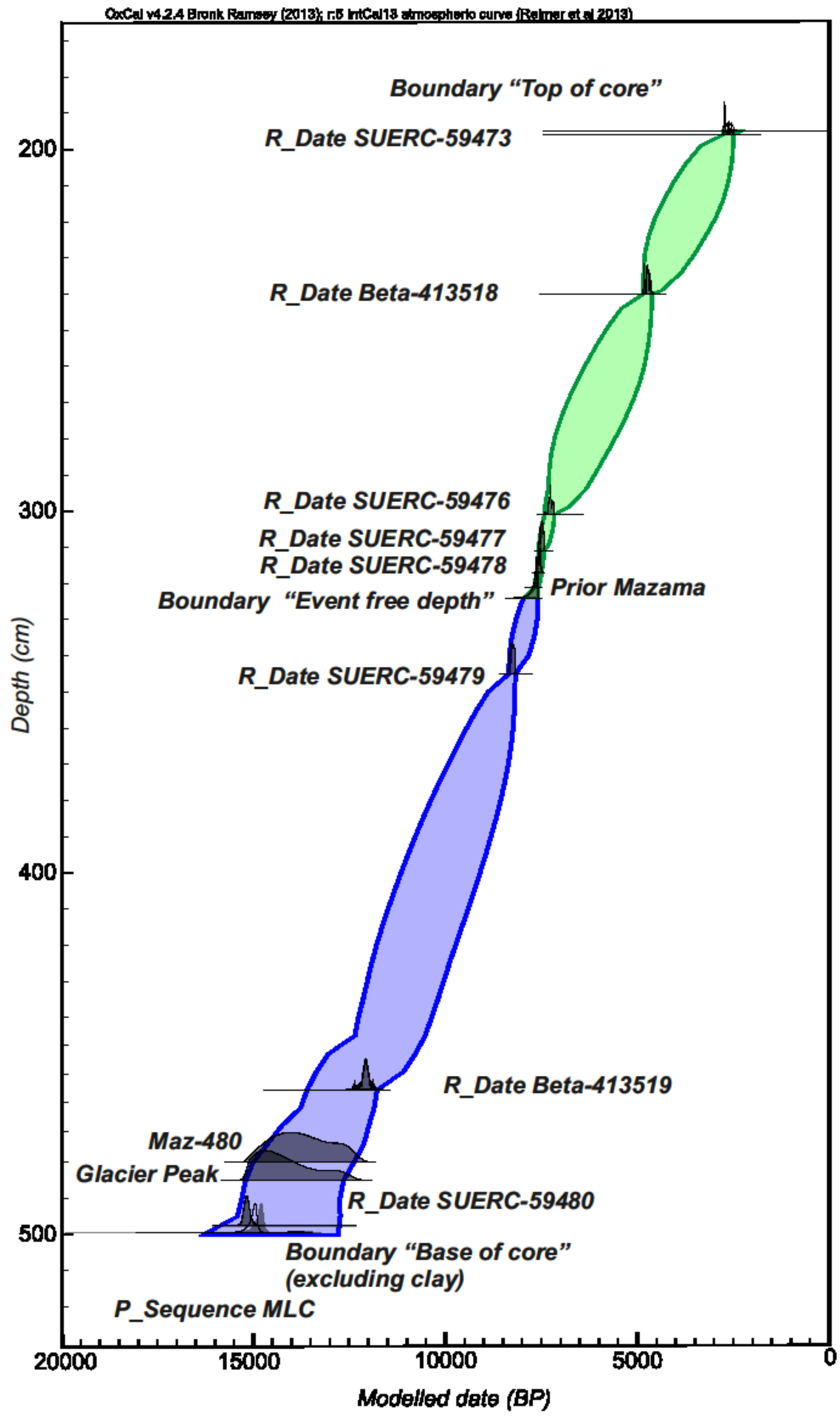

Figure 6: Bayesian age-depth (OxCal v.4.2 (Bronk Ramsey 2014)) model for MLC derived from the comparison of the radiocarbon ages calibrated using the IntCal13 (Reimer 2013) dataset.

Table 2: Conventional (^{14}C years BP) and calibrated (cal. years BP) radiocarbon ages for MLC and MLF, and modelled (at 95.4% probability range) radiocarbon ages for MLC.

Lab no.	Depth (cm)	Material	Age (^{14}C years BP ± 1 SD	Age range (cal. years BP 2 SD)	Modelled age (cal. years BP 95.4% probability range)
MLC					
SUERC-59473	200	Organic sediment	2561 ± 35	2755-2499	2759-2496
Beta-413518	240	Organic sediment	4200 ± 40	4849-4588	4844-4625
SUERC-59476	305	Organic sediment	6330 ± 36	7410-7167	7411-7166
SUERC-59477	315	Organic sediment	6590 ± 38	7565-7430	7564-7430
SUERC-59478	321	Organic sediment directly above MLC-T324	6687 ± 39	7619-7480	7619-7497
MLC-T324*	324	-	-	7682-7584*	7672-7582
SUERC-59479	345	Organic sediment	7430 ± 39	8344-8180	8346-8179
Beta-413519	460	Organic sediment	10,280 ± 40	12,374-11,827	13,599-11,774
MLC-T480**	480	-	-	-	15,009-12,379
MLC-T485**	485	-	-	-	15,204-12,645
SUERC-59480	495	Organic sediment	12,737 ± 50	15,346-14,980	15,419-12,737
Base of core (exc. Clay)**	500	-	-	-	16,294-12,789
MLF					
SUERC-52705	147	Organic sediment	5645 ± 36	6496-6319	-
SUERC- 55693	147 (re-submission)	Organic sediment	5796 ± 38	6713-6491	-
SUERC-52704	151	Organic sediment directly above MLF-T158	4948 ± 37	5745-5599	-
SUERC-55690	151 (re-submission)	Organic sediment directly above MLF-T158	5705 ± 35	6626-6407	-
SUERC-52703	161	Organic sediment below MLF-T158	7049 ± 41	7958-7795	-

*Age range from Egan et al. (2015)
** Age range based on deposition model

4.4. Vegetation record

4.4.1. MLC

The pollen record of MLC is shown in Figure 7 and summarised in Table 3. In zone MLCp-1 (~18,000-13,000 cal. years BP) *Pinus* diploxylon dominates. In zone MLCp-2 (13,000-7700 cal. years BP) *Pinus* diploxylon is replaced by *Pseudotsuga mensziesii* and *Alnus sinuata* increases until approximately 7900 cal. years BP when *Tsuga heterophylla* rapidly increases. In MLCp-3 (7700-2600 cal. years BP) *Tsuga heterophylla* dominates with an emergence of Cupressaceae and an increase of *Equisetum*.

Figure 8 focuses on the vegetation record above and below tephra deposits MLC-T485 and MLC-T480. *Pinus* diploxylon dominates throughout with percentages between 70% and 90%. Zonation was carried out on the section containing MLC-T485 (490-482 cm), revealing two zones (MLCg-1 (14,000-13,980 cal. years BP) and MLCg-2 (13,980-13,750 cal. years BP)), with a significant division within the assemblage prior to tephra deposition. The pollen record shows little difference in the assemblage before and after tephra deposition. Zonation was carried out separately on the section containing MLC-T480 (484-470 cm), revealing two zones (MLCm-1(13,750-13,420 cal. years BP) and MLCm-2 (13,420-13,140 cal. years BP)), with a significant division within the assemblage directly after tephra deposition. Figure 9 focuses on the vegetation record at the time MLC-T324 of deposition, which is the transition from zone MLCp-2 to MLCp-3 (Figure 7). Zonation was carried out on the assemblage around the time of tephra deposition (300-334 cm), revealing two zones displaying a clear division between the assemblage before and after tephra deposition. MLCt-1 (7780-7520 cal. years BP) is dominated by *Pseudotsuga menziesii* which shows an initial decreases after tephra deposition followed by a subsequent increase to a similar abundance as the pre-tephra levels. *Tsuga heterophylla,* Cupressaceae and *Alnus sinuata* all increase in abundance immediately after the tephra deposition, although this was short lived lasting approximately 50-80 years. MLCt-2 (7520-7100 cal. years BP) is dominated by *Pseudotsuga menziesii*. *Tsuga heterophylla* and Cupressaceae increase, and *Alnus sinuata decreases.* There is a brief peak in charcoal concentrations just after the tephra deposition.

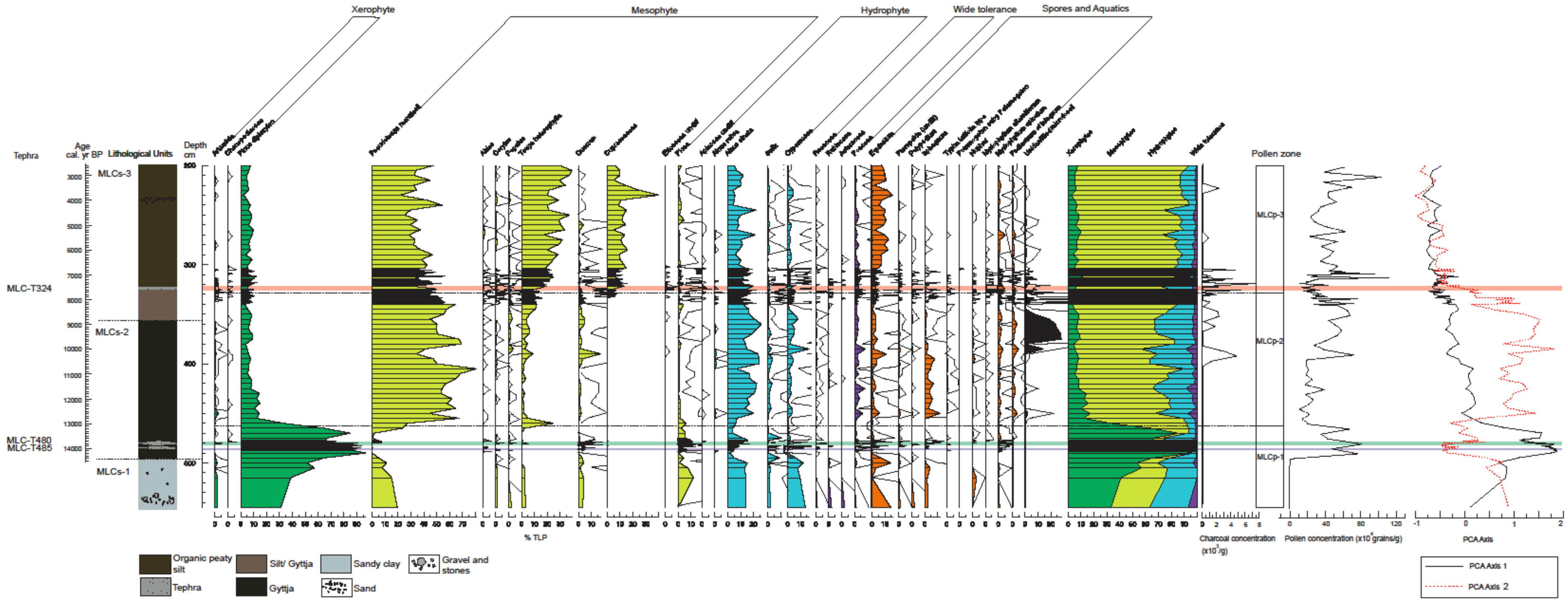

Figure 7: Late Pleistocene to early Holocene pollen assemblage of Moss Lake central displaying the age, lithology, percent of total land pollen, aquatics and macrophytes, summary diagram, pollen zonation, charcoal concentration, pollen concentration and PCA axis 1 and 2. The shaded bars represent the location of the tephra layers, also labelled. The solid line on percentage diagram is 10x exaggeration.

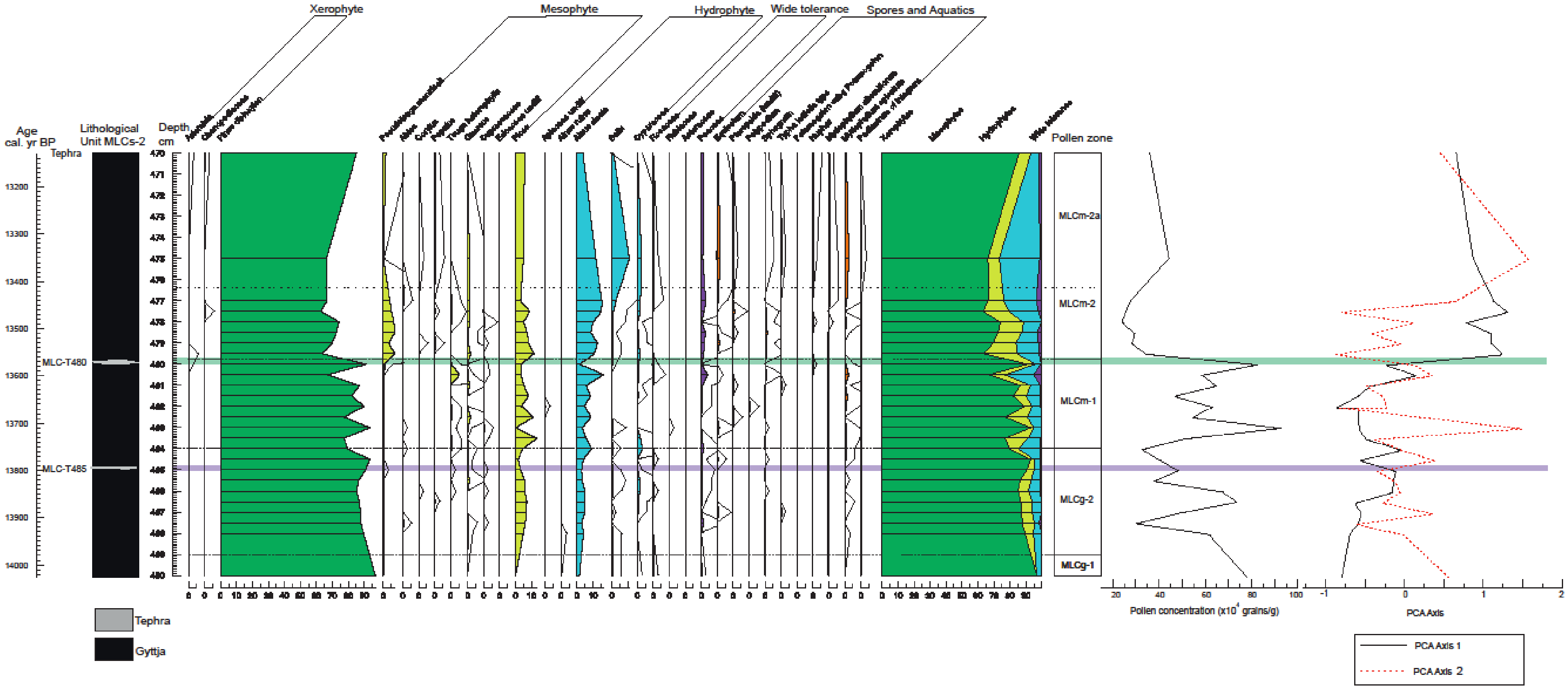

541

542 Figure 8: Pollen assemblage of Moss Lake central focussing on MLC-T485 and MLC-T480 tephra layers displaying the age, lithology,

543 percentage of total land pollen, aquatics and macrophytes, summary diagram, pollen zonation, charcoal concentration, pollen concentration and

544 PCA axis 1 and 2. The shaded bars represent the location of the tephra layers, also labelled. The solid line on percentage diagram is 10x

545 exaggeration.

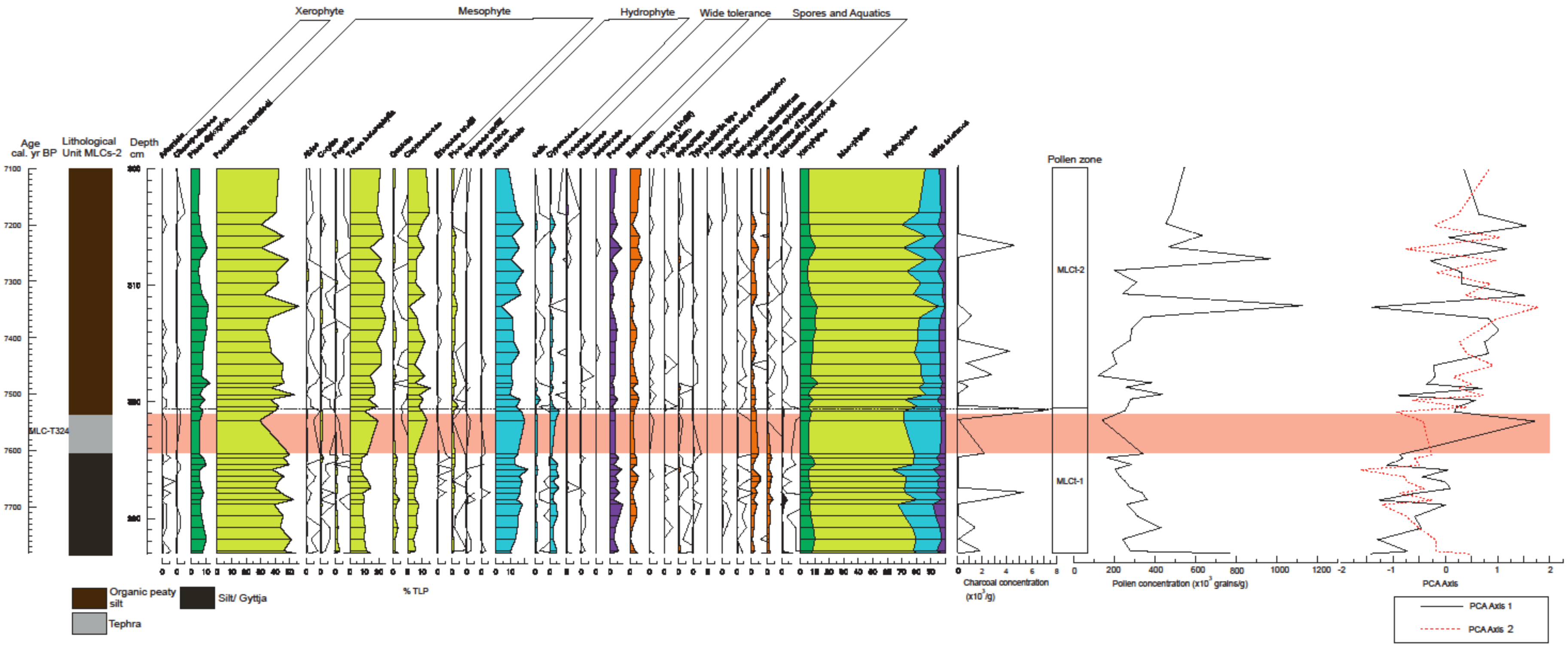

Figure 9: Pollen assemblage of Moss Lake central around the time of tephra deposition from the climactic eruption of Mount Mazama (MLC-T324) displaying the age, lithology, percent of total land pollen, aquatics and macrophytes, summary diagram, pollen zonation, charcoal concentration, pollen concentration and PCA axis 1 and 2. The shaded bar represents the location of the tephra layer, also labelled. The solid line on percentage diagram is 10x exaggeration.

4.4.2. MLF

Figure 10 focuses on the vegetation record at the time of MLF-T158 tephra deposition from the Moss Lake fringe core (MLF). Zonation indicated two zones with a significant division within the assemblage, although this occurs well after the tephra deposition (Table 3). MLFp-1 (160-150.9 cm) is dominated by *Pseudotsuga menziesii* and Cyperaceae. After tephra deposition Cyperaceae increases along with *Tsuga heterophylla* and *Pediastrum.* Many other taxa, including Poaceae and aquatics decline and disappear briefly such as *Myriophyllum spicatum* and *Nuphar.* Charcoal declines upon tephra deposition and remains low until 150.8 cm.

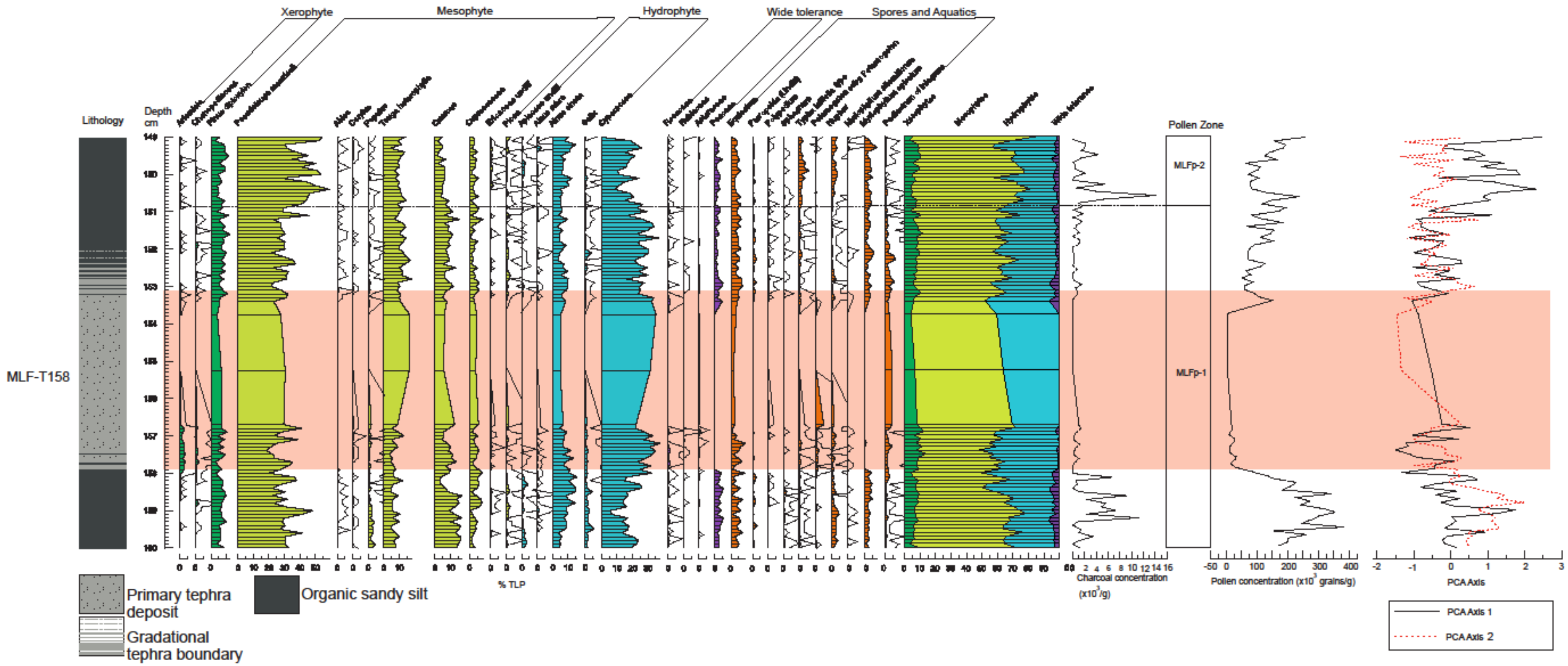

Figure 10: Pollen assemblage of Moss Lake fringe displaying the lithology, percent of total land pollen, aquatics and macrophytes, summary diagram, pollen zonation, charcoal concentration, pollen concentration and PCA axis 1 and 2. The shaded bar represents the location of MLF-T158, also labelled. The solid line on percentage diagram is 10x exaggeration.

Table 3: Pollen summary of Moss Lake central during the early to mid-Holocene, and during tephra deposition events from Glacier Peak (MLC-T485), Late Pleistocene Mazama (MLC-T480) and climactic Mazama (MLC-T324). The final summary is of the pollen assemblage from MLF with tephra from the climactic eruption of Mazama (MLF-T158).

Zone	**Depth (cm)**	**Pollen description**	**Pollen and charcoal concentration**
MLC- Early to mid-Holocene sequence			
MLCp-3	329-200	– Mesophytes remain dominant, particularly *Tsuga heterophylla* (up to 40%) – *Pseudotsuga menziesii* and *Alnus sinuata* slowly decrease. – Cupressaceae appears first in this zone. – *Equisetum* reaches its highest abundance.	Pollen concentration increases throughout. Charcoal peaks after tephra deposition.
MLCp-2	462-329	– Shift from xerophyte (*Pinus* diploxylon*)* dominance to mesophyte (*Pseudotsuga menziesii)* dominance. – *Tsuga heterophylla* increases (up to 20%). – Poaceae and *Sphagnum* reach their highest levels in this zone	Pollen concentration decreases. Charcoal concentration increases and fluctuates.
MLCp-1	545-462	– Dominated by *Pinus* diploxylon (up to 60%) – *Pseudotsuga menziesii* is in moderate abundance but disappears briefly. – *Alnus sinuata* is abundant but decrease around the time of Glacier Peak. – *Picea*, *Salix and Artemisia* are at their highest abundance in this zone.	Pollen concentration is high. Charcoal concentration is low.
MLC- Glacier Peak tephra deposition (MLC-T485)			
MLCg-2	489-484	– *Alnus sinuata* and *Picea* slightly increase through the zone and then decrease just before deposition. – *Pinus* diploxylon decreases. – After tephra deposition *Picea, Alnus sinuata* and Cyperaceae increase.	Pollen concentration decreases briefly around the time of tephra deposition.
MLCg-1	490-489	– *Pinus* diploxylon dominates, and steadily decreases throughout (up to 95%). – *Alnus sinuata* and *Picea* slowly increase but are in low abundance.	Pollen concentration is high.
MLC- Late Pleistocene Mazama tephra deposition (MLC-T480)			

MLCm-2	479.7-470	– *Pinus* diploxylon dominant (up to 90%) – *Alnus sinuata and Picea* steadily increase until sub zone m2a. – *Pseudotsuga menziesii* is abundant until sub zone m2a. – *Salix* increases in sub zone m2a.	Pollen concentration peaks just before tephra deposition, and then dramatically decreases.
MLCm-1	484-479.7	– *Pinus* diploxylon dominant (up to 95%). – *Alnus sinuata* and *Picea* are both in moderate abundance before tephra deposition and decrease upon it. – After tephra deposition *Pinus* diploxylon decrease to 60%, *Alnus sinuata and Picea* increase. – *Pseudotsuga menziesii* appears at the top of the zone.	Pollen concentration increases
MLC- Climactic Mazama tephra deposition (MLC-T324)			
MLCt-2	321-300	– After Mazama tephra deposition *Pseudotsuga menziesii* increases. – Cupressacae and *Alnus sinuata* decrease. – Vegetation dynamics are generally stable.	Pollen concentration increases. Charcoal decreases.
MLCt-1	333-321	– Mesophytes *Pseudotsuga menziesii* and *Tsuga heterophylla* dominate. – Upon tephra deposition *Pseudotsuga menziesii* decreases. – Cupressaceae, *Tsuga heterophylla and Alnus sinuata* increase. – *Pediastrum* almost disappears after tephra deposition but low throughout.	Pollen concentration decreases. Charcoal is variable, but peaks after tephra deposition.
MLF- Climactic Mazama tephra deposition (MLF-T158)			
MLFp-2	150.9-149	– Cyperaceae decreases to pre-tephra values of 10-20%. – *Pseudotsuga menziesii* and *Alnus sinuata* increase.	Pollen concentration increases to $16x10^3$/g, but is variable. Charcoal increases.
MLFp-1	162-150.9	– Before tephra deposition *Pseudotsuga menziesii* dominates (20-50%). – *Quercus* is in good abundance (10%), and decreases before tephra deposition. – Cyperaceae is in relatively low abundance towards the base of MLFp-1. – Upon tephra deposition Cyperaceae increase. – *Tsuga heterophylla* and *Quercus* increase upon tephra deposition, and *Alnus sinuata* decrease. – Poaceae, *Myriophyllum spicatum* and other aquatics disappear upon tephra deposition, and then return with the same abundance as pre-tephra values of <10% – *Pediastrum* increases upon tephra deposition	Pollen concentration is up to $11x10^3$/g, and drops to $1x10^3$/g after tephra deposition. Charcoal concentration reaches $10x10^3$/g before tephra, and declines to nearly 0 after.

569

4.5. Ordination and significance tests (PCA, variance partitioning and RDA)

4.5.1. Unconstrained ordination (PCA)

For the full Holocene record from MLC PCA axis 1 explains 49.7% of the variation. The positive scores for PCA axis 1 are driven by *Pinus* diploxylon and *Picea*, and the negative scores were driven by Cupressaceae, *Tsuga heterophylla*, *Pseudotsuga menziesii* and Cyperaceae. (Figure 11). PCA axis 1 is strongly positive in pollen zone MLCp-1, declines in pollen zone MLCp-2, and stabilises to become weakly negative in pollen zone MLCp-3 (Figure 7). For the biostratigraphic data containing MLC-T485 and MLC-T480 tephra PCA axis 1 explains 27% of the variation. The positive scores for PCA axis 1 are driven by *Pseudotsuga menziesii*, *Picea*, *Equisetum* and *Salix*, and the negative scores were driven by *Pinus diploxylon*, *Rubiaceae* and *Typha latifolia* (Figure 11). PCA axis 1 is strongly negative in pollen zone MLCg-1, increases in zones MLCg-2 and MLCm-1, then in MLCm-2 there is a shift to positive loadings which persists in MLCm-2a (Figure 8). PCA axis 1 for the MLC-T324 (climactic Mazama) data set in MLC accounted for 48% of the variation. The positive scores for PCA axis 1 are driven by *Tsuga heterophylla*, *Alnus sinuata*, Poaceae and Cupressaceae, and the negative scores were driven by *Pseudotsuga menziesii*, Cyperaceae and *Pediastrum* (Figure 11). PCA axis 1 loadings were negative in pollen zone MLCt-1, and upon tephra deposition they changed to strongly positive and then in zone MLCt-2 fluctuated between weakly negative and weakly positive scores (Figure 9). For the biostratigraphic data set containing MLF-T158 in MLF PCA axis 1 explains 60% of the variation. The positive scores for PCA axis 1 are driven by *Pseudotsuga menziesii*, *Tsuga heterophylla*, and Nuphar, and the negative scores were driven by Cyperaceae, *Quercus*, *Salix* and Cupressaceae (Figure 11). PCA axis 1 shifts from negative scores in pollen zone MLFp-1 to positive scores in zone MLFp-2 (Figure 10).

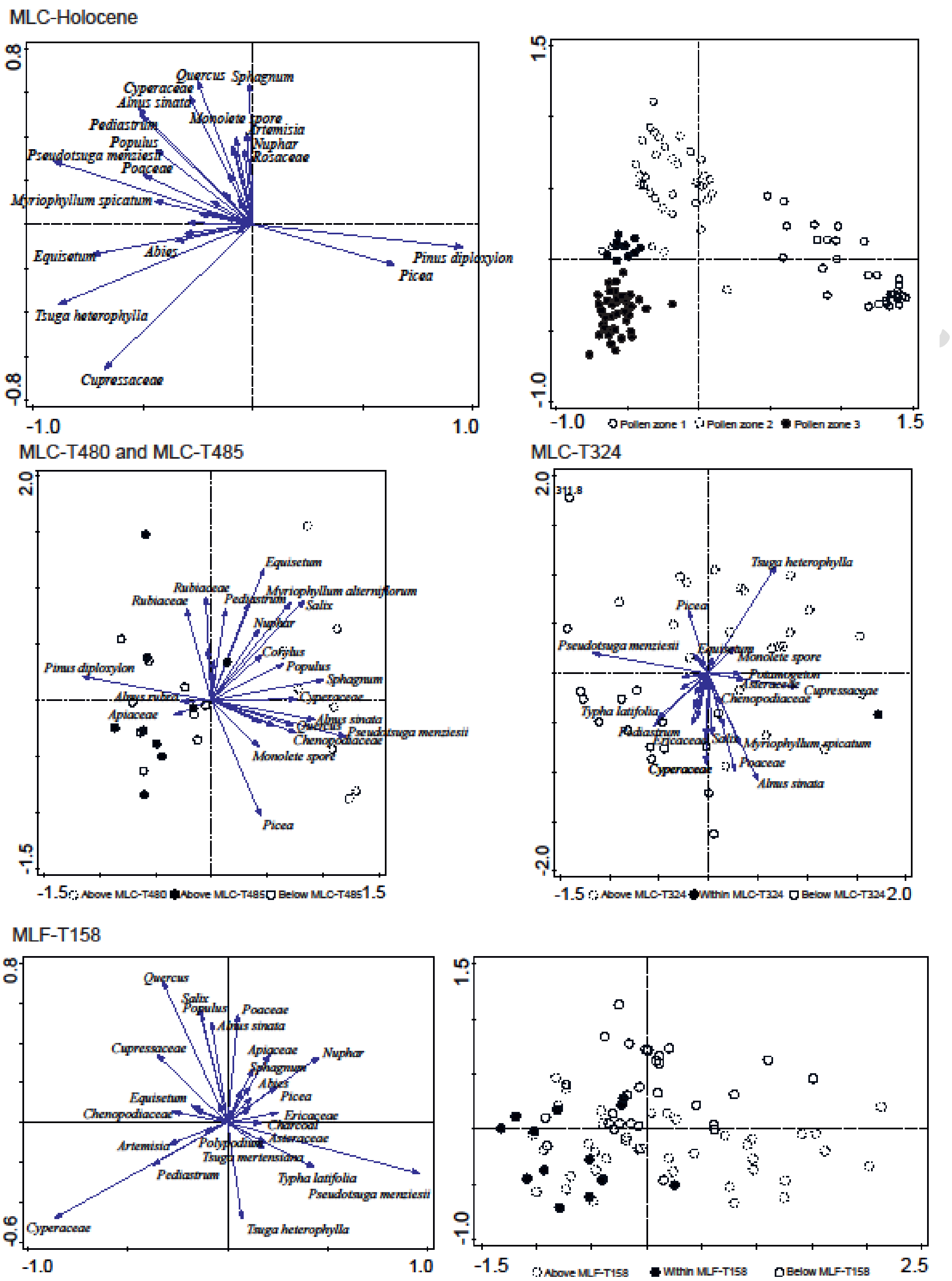

Figure 11: PCA score plots and bi-plots for the Holocene sequence from MLC and tephra biostratigraphies MLC-T485, MLC-T480, MLC-T324 and MLF-T158. PCA reported here is based on the percentage total pollen.

4.5.2. Constrained ordination

4.5.2.1. Variance partitioning

The results from the different variance partitioning models based on the different pollen sums are provided in Supplementary material C, Table 1. The results that were significant (p=<0.05) are highlighted. For the assemblage containing MLC-T480 the only significant variable was depth in the total pollen record (including aquatics and spores), arboreal pollen and concentration data sets. For MLC-T485 the models were all insignificant. Depth is the most important environmental variable for the assemblage MLC-T324 and was significant for all pollen sums but not in the concentration data. Tephra and LOI exerted no significant influence on this record. In the case of MLF, all environmental variables were significant for all pollen sums with the exception of tephra and the arboreal pollen record.

4.5.2.2. Redundancy analysis

Table 4 and Figure 12 display the results for partial redundancy analysis and associated significance tests for the biostratigraphic data sets that were significant in the previous variance partitioning models. The tephra variable is significantly important within six of the bisotratigraphic data sets from MLF explaining 11.6-40.4% of the variation, but not with arboreal pollen. The species most influenced by tephra seem to be the local species such as Cyperaceae, Poaceae and *Myriophyllum spicatum* in addition to *Artemisia,* however, the concentration data show the regional indicators to also be important such as *Pinus* diploxylon. The tephra variable is not significant in any of the biostratigraphic datasets for MLC-T324 and MLC-T480 in MLC. There is a significant relationship with depth in all three ashfalls. In MLF depth is significantly important in all bisostratigraphic datasets explaining 3-21.4% of the variation. For MLC-T324 in MLC depth is significant in all biostratigraphic datasets, except concentration, explaining 13.7-25.6% of the variation. Finally for MLC-

T480 depth was significantly important in the total pollen, arboreal and concentration datasets explaining 15.5-20.6% of the variation. The LOI variable which indicates pollen changes associated with sedimentological changes is significant in all six biostratigraphic datasets in MLF explaining 4.9-8.2% of the variations, but not in any of the data sets for MLC-T480 or MLC-T324.

Figure 12: RDA bi-plots for tephra biostratigraphies MLC-T485, MLC-T480, MLC-T324 and MLF-T158. Each bi-plot illustrates the relationship between diatom species and individual environmental variables. RDA reported here is based on the percentage total pollen.

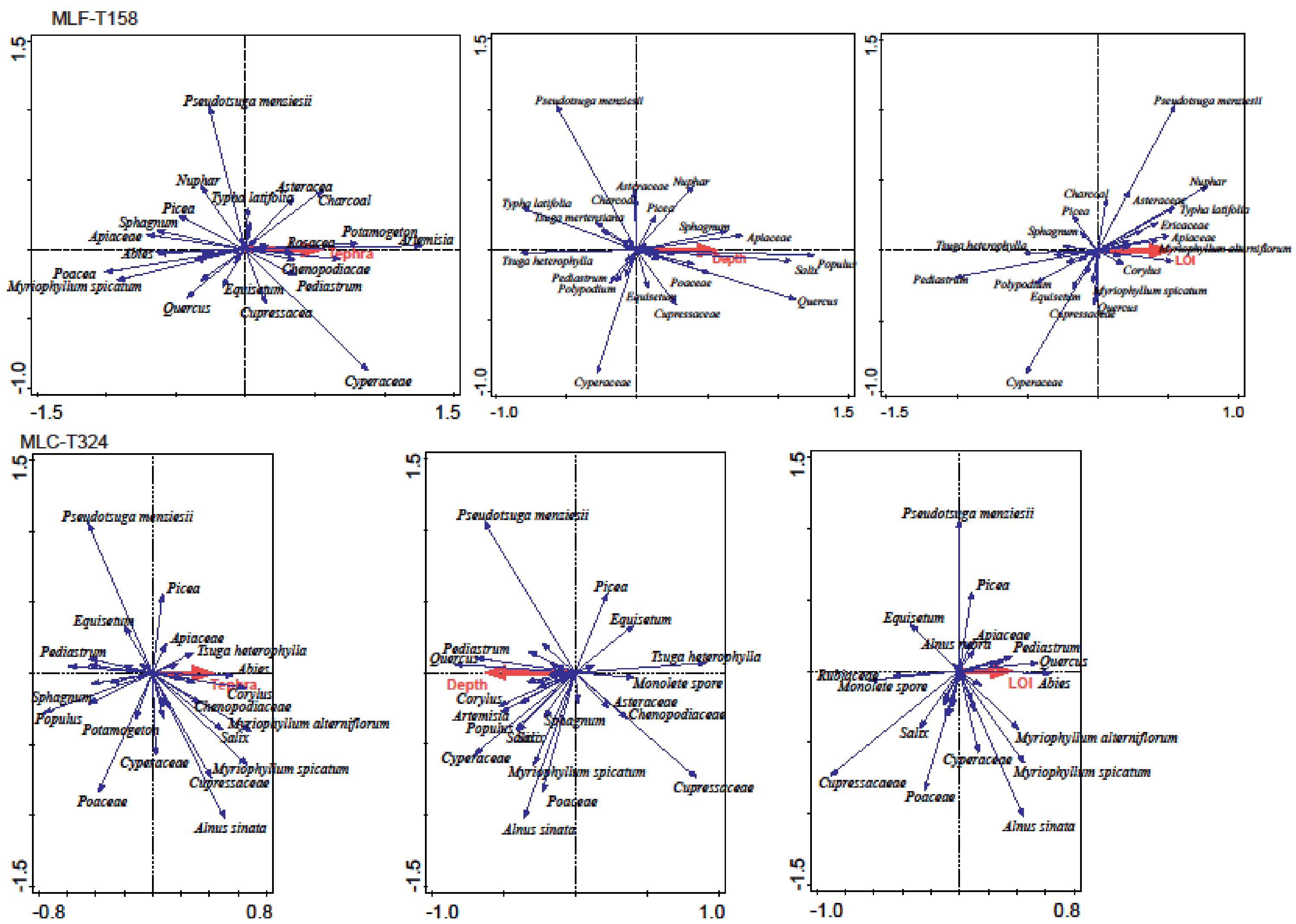

Table 4: Results of partial redundancy analysis (using the significant results from variance partitioning) of the pollen stratigraphical data sets of MLC-T324, MLC-T480 and MLF-T158 (MLC-T485 excluded due to insignificant results in variance partitioning) tephra layers for different models of explanatory variables and co-variables. Lower down the table is the percentage variation of the pollen, which indicates which species are most influenced by the variables. In this case only the pollen data for MLF have been presented as the RDA analyses from the central core revealed that tephra was an insignificant variable. The +/- signs means the species had either a positive or negative relationship with that particular variable. The shaded boxes show the analyses that had significant results (P= <0.05). Total pollen includes aquatics and spores.

RDA Results									
Variable	**Tephra**			**Depth**			**LOI**		
Co-variables	Depth + LOI			Tephra + LOI			Tephra + Depth		
	Significance of model	% explained by variable	Significance of variable	Significance of model	% explained by variable	Significance of variable	Significance of model	% explained by variable	Significance of variable
MLC-T324									
Total pollen	0.23	3.7	0.234	0.002	23.4	0.002	0.382	2.9	0.392
Arboreal pollen	0.208	3.9	0.224	0.002	25.6	0.002	0.322	3.2	0.338
Non-arboreal pollen	0.624	1.4	0.592	0.016	16.6	0.002	0.34	3	0.328
Wetland	0.748	0.8	0.712	0.004	16.8	0.004	0.762	0.8	0.716
Aquatics	0.132	5.5	0.122	0.01	13.7	0.004	0.366	2.9	0.406
MLC-T480									
Total pollen	0.342	8.3	0.286	0.016	18	0.014	0.194	9.5	0.206
Arboreal pollen	0.286	8.9	0.268	0.022	20.6	0.018	0.134	11.5	0.132
Concentration	0.094	10.6	0.082	0.01	15.5	0.006	0.814	5.2	0.788
MLF-T158									
Total pollen	0.002	11.6	0.002	0.002	12.1	0.002	0.006	6.8	0.004
Arboreal pollen	0.592	0.8	0.518	0.002	19.3	0.002	0.02	4.9	0.016
Non-arboreal pollen	0.002	13.5	0.004	0.022	5.5	0.022	0.012	8.1	0.01
Wetland	0.004	10.3	0.002	0.01	8	0.003	0.014	7.2	0.006
Aquatics	0.002	16.7	0.002	0.034	3	0.048	0.002	8.2	0.002
Concentration	0.002	40.4	0.002	0.002	21.4	0.002	0.004	7.3	0.004
% Variation of Pollen from RDA									

Variable Co-variables	**Tephra** Depth + LOI % Variation of pollen and relationship with variable	**Depth** Tephra + LOI % Variation of pollen and relationship with variable	**LOI** Tephra + Depth % Variation of pollen and relationship with variable
MLF-T158			
Total pollen	*Artemisia* (+50%) Cyperaceae (+24%) Poaceae (-31%) *Myriophyllum spicatum* (-26%)	*Populus* (+49%) *Tsuga heterophylla* (-21%) *Quercus* (+39%) *Salix* (+37%) *Typha latifolia* (-21%)	*Pediastrum* (-23%)
Arboreal pollen	-	*Populus* (+45%) *Tsuga heterophylla* (-20%) *Quercus* (+33%) Salix (+34%)	*Tsuga heterophylla* (-10%)
Non-arboreal pollen	*Artemisia* (+46%) Poaceae (-3%)	Poaceae (+11%)	Apiaceae (+13%)
Wetland	Apiaceae (-15%)	*Salix* (+42%)	Apiaceae (+10%)
Aquatics	*Myriophyllum spicatum* -(35%) *Potamogeton* (+26%)	*Typha latifolia* (-22%)	*Nuphar* (+16%)
Concentration	*Pinus* diploxylon (-42%) *Pseudotsuga menziesii* (-37%) *Tsuga heterophylla* (-35%) *Quercus* (-32%) Cupressaceae (-26) *Alnus sinuata* (-32%) Cyperaceae (+32%) Poaceae (-28%) *Equisetum* (-30%) *Myriophyllum alterniflorum* (-30%)	*Populus* (+49%) *Quercus* (+43%) Apiaceae (+36%) Poaceae (+29%)	*Pediastrum* (-12%)

5. Discussion

5.1.Late Pleistocene to mid-early Holocene environmental change at Moss Lake

The pollen record from MLC covers the time period between the Late Pleistocene and the mid-early Holocene allowing an evaluation of long term environmental change. The onset of the early Holocene was a time of a cool and dry environment, as indicated by the low pollen concentration and low LOI (cf. Grigg and Whitlock 1998; Walsh et al. 2008). The dominance of clays reflects the development of the lake as the clays are likely to be sourced from erosion of the surrounding area (Shuman, 2003). *Pinus* diploxylon was the first arboreal taxa to colonise the area due to its ability to inhabit the infertile soil and glacial till following deglaciation (Lotan and Critchfield, 1990). From around 12,000 cal. years BP the vegetation assemblage shifted to a closed mixed conifer forest dominated by *Pseudotsuga menziesii*, in response to warming, and relatively moist conditions. This trend in *Pseudotsuga menziesii*, has been observed in other parts of the Pacific Northwest (e.g. Barnosky, 1981, 1985; Courtney Mustaphi and Pisaric, 2014; Prichard et al. 2009) and is thought to be as a result of an amplification of solar radiation which intensified seasonality (Kutzbach, 1987; Whitlock, 1992). From 7600 cal. years BP the record indicates a further climate shift to a mild and wetter environment as indicated by the abundance of *Tsuga heterophylla* and Cupressaceae, consistent with regional trends (Gavin et al. 2011; Prichard et al. 2009; Walsh et al. 2008). Gavin et al. (2011) attributed the regional increase in *Tsuga heterophylla* to decreased continentality and increased winter moisture in the Interior Wet Belt region (valley bottoms in the Columbia and Rocky Mountains of southern British Columbia). Cupressaceae became increasingly more important from 5000 cal. years BP. Tesky (1992a) argued that this taxon is found as a codominant with *Tsuga heterophylla* in wet lowlands. These trends indicate the winters became significantly wetter and cooler during this period with dry summers (Walsh et al. 2008). The long-term vegetation record from Moss Lake is therefore consistent with the changes observed elsewhere in the Pacific Northwest (Courtney Mustaphi and Pisaric 2014; Prichard et al. 2009; Walsh et al. 2008; Whitlock, 1992).

5.2.Impact of tephra deposition

Classical palynological theory suggests there should be a different site-source relationships on the two cores with the fringe core most representative of local pollen and the central core most representative of regional pollen (Jacobson and Bradshaw 1981; Prentice 1985). The importance of the local vegetation signal in MLF is evidenced by the high abundance of Cyperaceae (30%) and aquatic pollen. The MLC record has a low proportion of Cyperaceae and aquatic pollen but a high percentage of arboreal pollen (~70%) indicative of a regional pollen signal.

5.2.1. Regional impact

MLC can be used to evaluate regional scale impacts and recovery of the tephra deposit from the climactic eruption of Mount Mazama. Additionally, the presence of other tephra deposits allows an assessment of the response to tephra falls of different magnitude. However, partial RDA shows no significant relationship between tephra and the different pollen biostratigraphies in all three of the tephra deposits identified in MLC, nor LOI. Conversely, partial RDA did show a significant relationship between depth and the different pollen biostratigraphies for all tephra deposits MLC-T324 (climatic eruption of Mazama) explaining 13.7-25.6% of the variation and MLC-T480 (Late Pleistocene eruption of Mazama) explaining 15.5-20.6% of the variation. The significant relationship with depth suggests the changes are probably associated with climate change.

During the time of the deposition of MLC-T480 there were significant climate changes ongoing. The timing of this deposition event was during the Pleistocene-Holocene transition and the expansion of the eastern Pacific subtropical-high pressure system of the Pacific Northwest (Bartlein et al. 1998; Whitlock, 1992), therefore major vegetation changes (reduction in *Pinus* diploxylon and increases in *Pseudotsuga menziesii* and *Picea*) around that time are likely to be explained by this change from a cold dry climate to a warmer and/or wetter climate, which is further evidence by partial RDA as these species had the highest percentage variations for the depth variable (25-28%). Zonation recognised the time of MLC-T480 as a point of significant change, as the boundary between MLCm-1 and MLCm-2 is on the tephra layer, however as partial redundancy analysis did not find a significant relationship with tephra it is likely that this is coincidence. This highlights the difficulty in distinguishing between tephra impacts and other forcing factors, and the importance of carrying out robust tests to determine the significance of tephra. The statistical tests using partial RDA are viewed as more robust, allowing for the conclusion that tephra deposition or the eruption itself did not have a statistically significant impact.

Focussing on the time of the deposition of MLC-T324, partial RDA revealed that the Mazama tephra had no statistically significant effect on the terrestrial environment, with depth (directional change) being found to be the most significant variable, explaining up to 25% of the variance. This suggests that changes in the assemblages are best attributed to ongoing environmental change, including climatic and ecological/successional factors. During this deposition event there are shifts in the vegetation assemblage with a decrease in *Pseudotsuga menziesii*, and an increase in Cupressaceae, *Tsuga heterophylla*, and *Alnus sinuata*, which thrive in moist environments (Tesky 1992a,b; Uchytil 1989), and are highlighted as important taxa in partial RDA with percentage variations of 38% for *Tsuga heterophylla*, 33% for Cupressaceae, 29% for *Alnus sinuata* and 19% for *Pseudotsuga menziesii*. This trend was observed regionally, specifically the increase of Cupressaceae and *Tsuga heterophylla* (Gavin et al. 2011; Prichard et al. 2009; Walsh et al. 2008), which as discussed in section 5.1 was due to decreased continentality and increased winter moisture in the Interior Wet Belt region (Gavin et al. 2011). It is important to note that these shifts started to occur just before tephra deposition and changed rapidly upon tephra deposition. Thus it is possible that tephra may have reinforced the ongoing changes. A possible mechanism for this could be that tephra influenced a change in sedimentology through water retention (Black and Mack, 1986), encouraging the development of peaty silts (Figure 3) coincident with the timing of tephra deposition and the *Tsuga heterophylla* increase, but as partial RDA showed no significant relationship of tephra and LOI with the biostratigraphic data it is not possible to demonstrate that tephra deposition had any influence.

5.2.2. Local impact

MLF can be used to evaluate local scale impacts and recovery of the tephra deposit from the climactic eruption of Mount Mazama (MLF-T158). Partial RDA revealed tephra to be a significant variable in all of the biostratigraphic data sets except arboreal pollen explaining 40-10.3% of the variation. The 40% variation came from the concentration data, however, as the concentration data is likely to have been impacted by a dilution effect of the tephra indicated by the low pollen concentrations (Figure 10 and Supplementary material D) this result is unreliable, and influx values cannot be precisely calculated given the dating resolution. Thus tephra significantly explained 10.3-16.7% of the variation. From the percentage data partial RDA indicated that *Artemisia*, Cyperaceae, Poaceae and *Myriophyllum spicatum* were the species most influenced by tephra deposition, and these species (except *Artemisia*) are also important in the concentration data (Table 4), suggesting that the Mazama tephra had a local impact on the open fringe vegetation and aquatic macrophytes. The importance of *Artemisia* should be taken with caution and is likely to be an artefact in the percentage data as the concentration data (Supplementary materials D) shows low concentrations throughout and is not an important species in the concentration partial RDA results.

The open fringe vegetation affected by tephra is Cyperaceae (+24%) and Poaceae (-31%). Cyperaceae responded positively to tephra deposition with pre-tephra values around 15-25% and post tephra values at 20-40%, and then returned to pre-tephra levels at 150.8 cm. This increase may reflect the adaptability of Cyperaceae to tephra deposition. Cyperaceae is a key taxa as an increase in sedges following Mazama ash deposition and deposition from other eruptions has been observed in other studies (e.g. Birks and Lotter, 1994; Lotter and Birks, 1993; Mehringer et al. 1977a), illustrating sedges survival mechanisms. Tephra could completely bury Cyperaceae species, but their individual survival mechanisms, such as perennial organs allowing shoots to erect through the tephra layer enable them to recover faster than other species (Antos and Zobel, 1985). However, the tephra deposit from Mazama is unlikely to have completely buried the Cyperaceae as the tephra layer is only 50 mm thick. Conversely, sedges often grow to create dense coverage on which the tephra can fall and create a blanket effect, reducing light, but their perennial organs will allow shoots to grow which could minimise the impact. This increase of sedges could also suggest that tephra caused increased water retention and surface wetness, as the tephra layer would have created an impermeable barrier in the soils reducing infiltration and also impeding drainage. Poaceae disappeared upon tephra deposition and returned after deposition with a slightly lower abundance than pre-tephra levels suggesting that this taxa were less able to adapt to tephra deposition. It is likely that Poaceae would have been buried by tephra, reducing gas exchange, light and its ability to photosynthesise.

The record shows a significant impact on the aquatic macrophytes affecting both emergent and submerged vegetation. Partial redundancy analysis revealed *Myriophyllum spicatum* to be negatively affected by tephra deposition and *Potamogeton* to be positively affected by tephra deposition, but qualitative analyses (Figure 10) suggest that aquatic impacts are also strongly indicated by *Equisetum* and *Pediastrum.* It is likely that *Myriophyllum spicatum, Equisetum* and *Nuphar* were affected by blanket burial causing the decline of the emergent taxa and a subsequent increase of turbidity within the lake would have caused the decrease of the submerged taxa due to a reduction in light availability. The decrease however was short lived as the aquatic macrophytes returned to pre-tephra levels. Also notable is the increase of *Potamogeton* and *Pediastrum.* The increase of these taxa suggest an increase in nutrient availability as *Potamogeton* require high nutrient levels (Lone et al. 2013) as does aquatic algae *Pediastrum*, which commonly increases after tephra deposition (Haberle et al. 2000) due to nutrient leaching. These nutrient rich conditions are also reflected by the orange colour of the Mazama tephra at MLF, as the colour suggests that the tephra has been weathered and would thus result in the release of Fe, Si and P (Jones and Gislason, 2008). Inspection of the glass shards confirm that the tephra has been weathered as vesicular shards from this deposit appear slightly yellow in colour, suggesting that the tephra was likely to have been deposited on the lake margin, likely above water level where oxidation could occur, with some having possibly been washed in from the surrounding area.

One concern about the interpretation of the data is the integrity of the stratigraphic record; a concern raised by the radiocarbon dates. The age reversal could be due to either sediment disturbance or contamination by humic acids. Mixing processes such as bioturbation, or wave action and post-depositional processes in the littoral zone could be the reason for the age reversal. Sediment mixing appears to be unlikely as there is no substantial stratigraphical evidence. The tephra layer present is intact suggesting that there was not enough mixing to completely re-work the tephra deposit, however, the possibility must be considered. Additionally, as the statistical tests evaluate the difference in the pollen assemblages above, below and within the tephra layer sediment mixing above the tephra layer would not compromise the analysis. Alternatively, contamination from humic acids that circulate in the silty peat sediment above the tephra layer could have caused the age reversal (Haberle and Bennett, 2004). Humic acids may exchange carbon or stick to sediments that have larger surface areas, such as the tephra and fine sand above the tephra, and may make those sediment ages too young. This process is called adsorption and is common in peats and organic muds (Higham, 2002) which are present in Moss Lake. Impacts below tephra are likely to be minimal due to the impermeable nature of the tephra.

Results from partial redundancy analysis indicate that the tephra effects are superimposed on other underlying environmental changes at the site as depth and LOI are both significantly important variables with depth explaining 3-21.4% of the variation and LOI explaining 4.9-8.2% of the variation. Considering the depth variable first it is mostly associated with changes in arboreal taxa: *Populus, Tsuga heterophylla* and *Quercus*, and some local taxa (*Typha latifolia* and Poaceae). *Populus* and *Quercus* decline discretely throughout the profile whilst *Tsuga heterophylla* increase suggesting a possible regional change associated with climate (discussed in section 5.1.), and local site changes reflecting by the general decrease of Poaceae and the increase of *Typha latifolia* throughout the profile. LOI is an indicator of local changes in sedimentology and partial RDA showed that it influences local taxa, particularly *Pediastrum*, which after its increase following tephra deposition declines throughout the rest of the profile, suggesting a reduction in sediment and nutrient delivery. The increase of *Typha latifolia* further indicates a local ongoing change as these are shade intolerant species and growth is restricted to sites following canopy opening but are otherwise tolerant of many other conditions (Gucker, 2008), which may reflect underlying changes locally at that time. Thus tephra did have a significant independent impact on the vegetation at the Moss Lake fringe location, but there were additional underlying trends associated with climatic and site specific changes.

5.2.3. Tephra effects on fire

A secondary impact of volcanic eruptions is an increase in thunderstorms (Beierle and Smith, 1998; Thorarinsson, 1979). This is because, explosive eruptions emit large volumes of fine and very fine tephra that can travel further distances and have the most positive charge, meaning lightening could occur more frequently whilst there is tephra in the atmosphere (McNutt and Davis, 2000). A further consideration is the effect of tephra on fire history. If increased lightening occurred during the time of the Mount Mazama eruption and subsequent tephra dispersal it is possible that some trees may have been struck by lightning; an ignition source for forest fires. It is likely that forest fires were occurring before Mazama tephra deposition, as indicated in both the MLC and MLF record. During the time of tephra deposition charcoal levels from MLC show evidence for increased regional fires. The local record from MLF shows a reduction of local forest fires after tephra deposition. However, such a phenomenon usually occurs proximal to the volcano, so is unlikely to be the reason for the increased charcoal levels, but cannot be discounted due to the large volume of ash emitted and transported. The peak observed in MLC after tephra deposition is possibly due to the influx of charcoal into the lake from distal areas, tens of km away from the site (Patterson et al. 1987), where regionally, forest fires may have occurred as an effect of the eruption. The lack of macro-charcoal, and low values of micro-charcoal at the lake edge site, MLF, indicates there were no forest fires in the catchment area of Moss Lake.

5.3.Implications for future research

This study has evidenced the importance of evaluating impacts based on central basin and fringe cores, as it is evident from this study that a single core from the centre of Moss Lake would have revealed no tephra impact, so future research should aim to collect cores with different pollen source areas (Jacobson and Bradshaw 1981; Prentice 1985). The fringe core revealed significant impacts of tephra deposition, however, there are uncertainties as to how representative this effect is of the wider region. There are several factors that might affect the response to tephra and must be considered in future studies. The first is to consider how different receiving environments might respond. Moss Lake is in a closed conifer forest with little understorey vegetation, which suggests that it may be resilient to disturbance, but if the receiving environment was ecologically stressed in some way, such as conifer trees starting to decline, then the impact could be much more adverse and contribute to a complete community re-structure. The vulnerability and sensitivity of specific vegetation types to tephra deposition is also important, as it has been found that understorey species are most adversely affected (Hotes et al. 2006; Millar et al. 2006).

Another key point to consider is how close to the volcano the study area needs to be to observe a significantly long-term effect on the terrestrial environment. This is in part linked to the tephra layer thickness as it has been found that thicker tephra layers impact more adversely (Antos and Zobel, 2005), and are likely to be thicker closer to the source but it is unknown what the minimum tephra thickness is to see a substantial impact on the environment. Although a 50 mm tephra deposit had an impact on local vegetation at Moss Lake this impact may not be representative of other sites, thus these issues of tephra thickness, distance from the source and how representative one site is of the wider region are still unresolved. In addition, this study was unable to determine the duration of the observed impacts due to the lack of a well constrained chronology. Future studies should aim to resolve these issues.

A final control is natural variability. It is attracting to assume that a "wiggle" coincident with a tephra layer is reflective of an impact, but it is not possible to fully understand impacts of tephra without considering underlying trends. Despite the short-term impact that tephra can have on terrestrial ecosystems, overall long-term climate and ecological changes are likely to exert most control (Long et al. 2011), and so it is necessary to gain an understanding of the climate and successional changes that were ongoing during the time of a volcanic event.

There are other important considerations for future studies regarding the deposition and re-working of the tephra layer. Firstly, tephra can have a patchy distribution, "*assumptions of blanket-like deposition cannot be justified*" (Boygle, 1999:146). Meteorological influences on plume dynamics can limit tephra dispersal. For example, during dry, calm anti-cyclonic weather there will be an increase in particle concentration in the atmosphere (Grattan and Pyatt, 1994) and this will produce blanket-like deposition of tephra, while precipitation bearing systems produce a sporadic and discontinuous pattern (Boygle, 1999). In addition, clustering in the atmosphere can prevent uniform deposition of tephra over a wide area (Lawson et al. 2012). This might explain why a regional impact was not detected.

Another potential issue with such studies is the possibility that tephra layers are re-worked by mixing processes such as bioturbation or become displaced within the sediment. Tephra can move vertically and horizontally through liquefied sediment if the density of the tephra is greater than the density of the sediment. This is termed stratigraphic displacement and has been reported in similar organic lake sediments (Anderson et al. 1984; Beierle and Bond, 2002). Down-core relocation of Mazama tephra has been reported in sediment cores from Copper Lake, Alberta, which suggest that the tephra layer moved down-core by the equivalent of more than 3000 years (Beierle and Bond, 2002). However, we deem this process as unlikely in Moss Lake, where no evidence for relocations was seen, e.g. entrainment of small quantities of gyttja within the tephra layer (Beierle and Bond, 2002) These secondary factors are important to consider for other impact studies and may challenge tephrochronological applications.

6. Conclusion

Central and fringe cores were taken from Moss Lake containing tephras from Glacier Peak (MLC-T485), Late Pleistocene Mazama tephra (MLC-T480), and a mid-Holocene (climactic eruption) Mazama tephra (MLC-T324, MLF-T158). High resolution pollen analyses, stratigraphic analyses and detailed statistics (PCA, variance partitioning and partial RDA) were able to determine if these tephra deposits had an impact on the terrestrial and aquatic ecosystem at a regional and local scale. There is evidence of local impacts of the climactic eruption of Mazama (MLF-T158). The record reveals an impact on open vegetation and aquatic macrophytes with a decrease of Poaceae but an increase of Cyperaceae, which reflects this taxa's ability to adapt and its positive response to increased surface wetness. Aquatic macrophytes generally decreased after tephra deposition due to blanket burial and increasing the turbidity of the water reducing light for the submerged taxa, ultimately leading to a reduced ability to photosynthesise. The impacts were short term but their persistence cannot be currently quantified due to limited dating control. In contrast there is no statistically significant impact of tephra recorded from Moss Lake central (MLC), indicating minimal impact on regional forest composition. Overall, the vegetation change associated with such a significant tephra fall is highly restricted compared to long-term changes during the Holocene period. Furthermore, there was no significant impact of tephra deposition from the thinner tephra falls MLC-T485 (Late Pleistocene Mazama) and MLC-T480 (Glacier Peak). Future studies need to assess the impacts of ash falls on both local and regional scales, and must be aware of the resilience of the particular environment in question and consider the thickness of the tephra layer, and ongoing environmental changes as a control on the observed response.

7. Acknowledgements

This work was supported by the NERC Radiocarbon Facility NRCF010001 (allocation numbers 1877.1014; 1728.1013). Fieldwork was partially funded by the Royal Geographical Society with IBG (Geographical Club Award Ref. 03.13). We thank Vicki Smith at The University of Oxford for EPMA, and Danielle Alderson (The University of Manchester) and Harold N. Wershow (Western Washington University) for assistance in the field. Finally, we thank Pete Ryan and the two anonymous reviewers for useful comments on the manuscript.

References

Abella, S.E., (1988) The effect of Mt. Mazama ashfall on the planktonic diatom community of Lake Washington. *Limnology and oceanography*, 33(6), 1376–1385.

Anderson, R.Y., Nuhfer, E.B. & Dean, W.E., (1984) Sinking of volcanic ash in uncompacted sediment in williams lake, washington. *Science*, 225(4661), 505–8.

Antos, J.A. & Zobel, D.B., (1985) Plant form, developmental plasticity, and survival following burial by volcanic tephra. *Canadian Journal of Botany*, 63(12), 2083–2090.

Antos, J.A. & Zobel, D.B., (2005) Plant repsonses in forests of the tephra-fall zone. In V. H. Dale, F. J. Swanson, & C. M. Crisafulli, eds. *Ecological Responses to the 1980 Eruption of Mount St. Helens*. New york: Springer, pp. 47–58.

Bacon, C.R., (1983) Eruptive history of Mount Mazama and Crater Lake Caldera, Cascade Range, U.S.A. *Journal of Volcanology and Geothermal Research*, 18(1-4), 57–115.

Barker, P., Telford, R., Merdaci, O., Williamson, D., Taieb, M., Vincens, A. & Gibert, E., (2000) The sensitivity of a Tanzanian crater lake to catastrophic tephra input and four millennia of climate change. *The Holocene*, 10(3), 303–310.

Barnosky, C.W., (1981) A record of late Quaternary vegetation from Davis Lake, southern Puget Lowland, Washington. *Quaternary Research*, 16(2), 221–239.

Barnosky, C.W., (1985) Late Quaternary vegetation in the Southwestern Columbia Basin, Washington. *Quaternary Research*, 23(1), 109–122.

Bartlein, P., Anderson, K., Anderson, P., Edwards, M., Mock, C., Thompson, R., Webb, R., Webb III, T. & Whitlock, C., (1998) Paleoclimate simulations for North America over the past 21,000 years. *Quaternary Science Reviews*, 17(6-7), 549–585.

Beierle, B. & Bond, J., (2002) Density-induced settling of tephra through organic lake sediments. *Journal of Paleolimnology*, 28(4), 433–440.

Beierle, B. & Smith, D.G., (1998) Severe drought in the early Holocene (10,000–6800 BP) interpreted from lake sediment cores, southwestern Alberta, Canada. *Palaeogeography, Palaeoclimatology, Palaeoecology*, 140(1-4), 75–83.

Bennett, K.D., (1996) Determination of the number of zones in a biostratigraphical sequence. *New Phytologist*, 132(1), 155–170.

Bennett, K.D., (2007) Psimpoll and Pscomb programs for plotting and analysis. Available from: http://www.chrono.qub.ac.uk/psimpoll/psimpoll.html [Last accessed: 18/02/2015]

Birks, H.J.B. & Birks, H.H., (1980) *Quaternary palaeoecology*, London: Arnold Press.

Birks, H.J.B. & Lotter, A.F., (1994) The impact of the Laacher See Volcano (11 000 yr B.P.) on terrestrial vegetation and diatoms. *Journal of Paleolimnology*, 11(3), 313–322.

Black, R.A. & Mack, R.N., (1984) Aseasonal leaf abscission in Populus induced by volcanic ash. *Oecologia*, 64(3), 295–299.

Black, R.A. & Mack, R.N., (1986) Mount St. Helens Ash: Recreating Its Effects on the

Steppe Environment and Ecophysiology. *Ecology*, 67(5), 1289.

Blackford, J.J., Edwards, K.J., Dugmore, A.J., Cook, G.T. & Buckland, P.C., (1992) Icelandic volcanic ash and the mid- Holocene Scots pine (*Pinus sylvestris*) pollen decline in northern Scotland. *The Holocene*, 2(3), 260–265.

Blackford, J.J., Payne, R.J., Heggen, M.P., de la Riva Caballero, A. & van der Plicht, J., (2014) Age and impacts of the caldera-forming Aniakchak II eruption in western Alaska. *Quaternary Research*, 82(1), 85–95.

Blinman, E., Mehringer, P.J. & Sheppard, J.C., (1979) Pollen influx and the deposition of Mazama and Glacier Peak tephra. In P. Sheets & D. Grayson, eds. *Volcanic Activity and Human Ecology*. London: Academic Press Inc, pp. 393–425.

Borcard, D., Legendre, P. & Drapeau, P., (1992) Partialling out the Spatial Component of Ecological Variation. *Ecology*, 73(3), 1045.

Boygle, J., (1999) Variability of tephra in lake and catchment sediments, Svínavatn, Iceland. *Global and Planetary Change*, 21(1-3), 129–149.

ter Braak, C. & Prentice, I., (1988) *A theory of gradient analysis*, London: Academic Press Inc.

ter Braak, C. & Šmilauer, P., (2012) *Canoco reference manual and user's guide: software for ordination, version 5.0.*, Ithaca, USA: Microcomputer Power.

Brockman, F.C., (1968) *Trees of North America*, New york: Golden Press.

Broecker, W.S., Kulp, J.L. & Tucek, C.S., (1956) Lamont Natural Radiocarbon Measurements III. *Science (New York, N.Y.)*, 124(3223), 630.

Bronk Ramsey, C., (2014) OxCal V. 4.2. Available from:

https://c14.arch.ox.ac.uk/oxcal/OxCal.html [Last accessed: 20/11/2015]

Caseldine, C., Hatton, J., Huber, U., Chiverrell, R. & Woolley, N., (1998) Assessing the impact of volcanic activity on mid-Holocene climate in Ireland: the need for replicate data. *The Holocene*, 8(1), 105–111.

Chakraborty, P., Raghunadh Babu, P. V, Acharyya, T. & Bandyopadhyay, D., (2010) Stress and toxicity of biologically important transition metals (Co, Ni, Cu and Zn) on phytoplankton in a tropical freshwater system: An investigation with pigment analysis by HPLC. *Chemosphere*, 80(5), 548–53.

Cook, R.J., Barron, J.C., Papendick, R.I. & Williams, G.J., (1981) Impact on agriculture of the mount st. Helens eruptions. *Science (New York, N.Y.)*, 211(4477), 16–22.

Courtney Mustaphi, C.J. & Pisaric, M.F.J., (2014) Holocene climate–fire–vegetation interactions at a subalpine watershed in southeastern British Columbia, Canada. *Quaternary Research*, 81(2), 228–239.

Dearing, J., (1994) *Environmental Magnetic Susceptibility: Using the Bartington MS2 System.*, Kenilworth: Chi Publishing.

Delmelle, P., Stix, J., Baxter, P., Garcia-Alvarez, J. & Barquero, J., (2002) Atmospheric dispersion, environmental effects and potential health hazard associated with the low-altitude gas plume of Masaya volcano, Nicaragua. *Bulletin of Volcanology*, 64(6), 423–434.

Delmelle, P., Stix, J., Bourque, C.P., Baxter, P.J., Garcia-Alvarez, J. & Barquero, J., (2001) Dry deposition and heavy acid loading in the vicinity of Masaya Volcano, a major sulfur and chlorine source in Nicaragua. *Environmental science & technology*, 35(7), 1289–93.

Dragovich, J.D. et al., (2002) *Geological map of Washington- Northwest Quadrant: Washington Division of Geology and Earth Resources Geological Map GM-50, 3 sheets, scale 1:250,000*, pp.1-80.

Egan, J., Staff, R.A. & Blackford, J., (2015) A revised age estimate of the Holocene Plinian eruption of Mount Mazama, Oregon using Bayesian statistical modelling. *The Holocene*, 25(7), 1054–1067.

Frenzen, P., (2000) USDA: Mount St. Helens National Volcanic Monument. *What is the status of plant recovery 25 years after the eruption?* Available from: http://www.fs.usda.gov/wps/portal/fsinternet/!ut/p/c4/04_SB8K8xLLM9MSSzPy8xBz9CP0os3gDfxMDT8MwRydLA1cj72DTUE8TAwjQL8h2VAQAMtzFUw!!/?navtype=BROWSEBYSUBJECT&cid=stelprdb5200174&navid=150130000000000&pnavid=150000000000000&ss=110623&position=Welcome*&ttype= [Last accessed: 10/10/2015]

Gavin, D.G., Henderson, A.C.G., Westover, K.S., Fritz, S.C., Walker, I.R., Leng, M.J. & Hu, F.S., (2011) Abrupt Holocene climate change and potential response to solar forcing in western Canada. *Quaternary Science Reviews*, 30(9-10), 1243–1255.

Giles, T.M., Newnham, R.M., Lowe, D.J. & Munro, A.J., (1999) Impact of tephra fall and environmental change: a 1000 year record from Matakana Island, Bay of Plenty, North Island, New Zealand. *Geological Society, London, Special Publications*, 161(1), 11–26.

Grattan, J.P. & Pyatt, F.B., (1994) Acid damage to vegetation following the Laki fissure eruption in 1783 — an historical review. *Science of The Total Environment*, 151(3), 241–247.

Grigg, L.D. & Whitlock, C., (1998) Late-Glacial Vegetation and Climate Change in Western Oregon. *Quaternary Research*, 49(3), 287–298.

Grishin, S.Y., Moral, R., Krestov, P. V. & Verkholat, V.P., (1996) Succession following the catastrophic eruption of Ksudach volcano (Kamchatka, 1907). *Vegetatio*, 127(2), 129–153.

Gucker, C.L., (2008) Typha latifolia. In: Fire Effects Information System, [Online]. *U.S. Department of Agriculture, Forest Service, Rocky Mountain Research Station, Fire Sciences Laboratory (Producer).* Available from: http://www.fs.fed.us/database/feis/plants/graminoid/typlat/all.html [Last accessed: 28/01/2016].

Haberle, S., Szeicz, J. & Bennett, K., (2000) Late Holocene vegetation dynamics and lake geochemistry at Laguna Miranda, XI Region, Chile Dinámica vegetaciónal y geoquímica lacustre del Holoceno. *Revista Chilena de historia natural*, 73(4), 1–5.

Haberle, S.G. & Bennett, K.D., (2004) Postglacial formation and dynamics of North Patagonian Rainforest in the Chonos Archipelago, Southern Chile. *Quaternary Science Reviews*, 23(23-24), 2433–2452.

Hall, V.A., (2003) Assessing the impact of Icelandic volcanism on vegetation systems in the north of Ireland in the fifth and sixth millennia BC. *The Holocene*, 13(1), 131–138.

Hall, V.A., Pilcher, J.R. & McCormac, F.G., (1994) Icelandic volcanic ash and the mid-Holocene Scots pine (Pinus sylvestris) decline in the north of Ireland: no correlation. *The Holocene*, 4(1), 79–83.

Hallett, D.J., Mathewes, R.W. & Foit, F.F., (2001) Mid-Holocene Glacier Peak and Mount St. Helens We Tephra Layers Detected in Lake Sediments from Southern British Columbia Using High-Resolution Techniques. *Quaternary Research*, 55(3), 284–292.

Heinrichs, M.L., Walker, I.R., Mathewes, R.W. & Hebda, R.J., (1999) Holocene chironomidinferred salinity and paleovegetation reconstruction from Kilpoola Lake, British Columbia. *Géographie physique et Quaternaire,* 53(2), 211–221.

Heusser, L.E. & Stock, C.E., (1984) Preparation techniques for concentrating pollen from marine sediments and other sediments with low pollen density. *Palynology*, 8(1), 225–227.

Higham, T.F.G., (2002) Web-info Radiocarbon. Available from: http://www.c14dating.com/pret.html [Last accessed: 27/11/2015]

Hildreth, W. & Fierstein, J., (1997) Recent eruptions of Mount Adams, Washington Cascades, USA. *Bulletin of Volcanology*, 58(6), 472–490.

Hill, M. & Gauch, H., (1980) Detrended correspondence analysis: an improved ordination technique. *Vegetatio*, 42, 47–58.

Hinckley, T.M. et al., (1984) Impact of tephra deposition on growth in conifers: the year of the eruption. *Canadian Journal of Forest Research*, 14(5), 731–739.

Hotes, S., Poschlod, P., Sakai, H. & Inoue, T., (2001) Vegetation, hydrology, and development of a coastal mire in Hokkaido, Japan, affected by flooding and tephra deposition. *Canadian Journal of Botany*, 79(3), 341–361.

Hotes, S., Poschlod, P. & Takahashi, H., (2006) Effects of volcanic activity on mire development: Case studies form Hokkaido, northern Japan. *The Holocene*, 16, 561–573.

Hotes, S., Poschlod, P., Takahashi, H., Grootjans, A.P. & Adema, E., (2004) Effects of tephra deposition on mire vegetation: a field experiment in Hokkaido, Japan. *Journal of Ecology*, 92(4), 624–634.

Jacobson, G.L. & Bradshaw, R.H.W., (1981) The selection of sites for paleovegetational studies. *Quaternary Research*, 16(1), 80–96.

Jochum, K.P. & Nohl, U., (2008) Reference materials in geochemistry and environmental research and the GeoReM database. *Chemical Geology*, 253(1-2), 50–53.

Jones, M. & Gislason, S., (2008) Rapid releases of metal salts and nutrients following the deposition of volcanic ash into aqueous environments. *Geochimica et Cosmochimica Acta*, 72(15), 3661–3680.

Kilian, R., Biester, H., Behrmann, J., Baeza, O., Fesq-Martin, M., Hohner, M., Schimpf, D., Friedmann, A. & Mangini, A., (2006) Millennium-scale volcanic impact on a superhumid and pristine ecosystem. *Geology*, 34(8), 609–612.

Kuehn, S.C. & Foit, F.F., (2006) Correlation of widespread Holocene and Pleistocene tephra layers from Newberry Volcano, Oregon, USA, using glass compositions and numerical analysis. *Quaternary International*, 148(1), 113–137.

Kuehn, S.C., Froese, D.G., Carrara, P.E., Foit, F.F., Pearce, N.J.G. & Rotheisler, P., (2009) Major- and trace-element characterization, expanded distribution, and a new chronology for the latest Pleistocene Glacier Peak tephras in western North America. *Quaternary Research*, 71(2), 201–216.

Kutzbach, J.E., (1987) Model simulations of the climatic patterns during the deglaciation of North America. In W. F. Ruddiman & H. . Wright Jr, eds. *North America and adjacent oceans during the last deglaciation.* Boulder, Colorado: Geological Society of America, pp. 425–446.

Lallement, M., Macchi, P.J., Vigliano, P., Juarez, S., Rechencq, M., Baker, M., Bouwes, N. & Crowl, T., (2016) Rising from the ashes: Changes in salmonid fish assemblages after 30months of the Puyehue-Cordon Caulle volcanic eruption. *The Science of the total* *environment*, 541, 1041–51.

Lawson, I.T., Swindles, G.T., Plunkett, G. & Greenberg, D., (2012) The spatial distribution of Holocene cryptotephras in north-west Europe since 7 ka: implications for understanding ash fall events from Icelandic eruptions. *Quaternary Science Reviews*, 41, 57–66.

Leopold, E.B., Nickmann, R., Hedges, J.I. & Ertel, J.R., (1982) Pollen and lignin records of late quaternary vegetation, lake washington. *Science (New York, N.Y.)*, 218(4579), 1305–7.

Leps, J. & Smilauer, P., (2014) *Multivariate analysis of ecological data using CANOCO 5* 2nd ed., Cambridge: Cambridge University Press.

Lone, P., Bhardwaj, A. & Bahar, F., (2013) A study of comparative purification efficiency of two species of Potamogetón (Submerged Macrophyte) in wastewater treatment. *International Journal of Scientific and Research Publications*, 3(1), 1–5.

Long, C.J., Power, M.J. & Bartlein, P.J., (2011) The effects of fire and tephra deposition on forest vegetation in the Central Cascades, Oregon. *Quaternary Research*, 75(1), 151–158.

Long, C.J., Power, M.J., Minckley, T.A. & Hass, A.L., (2014) The impact of Mt Mazama tephra deposition on forest vegetation in the Central Cascades, Oregon, USA. *The Holocene*, 24(4), 503–511.

Lotan, J.E. & Critchfield, W.B., (1990) Silvics of North America: Volume 1 Conifers-Lodgepole Pine. *Agriculture Handbook 654, U.S. Dept. of Agriculture, Forest Service, Washington, D.C.*, 2, 877.

Lotter, A. & Birks, H., (1993) The Impact of the Laacher See Tephra on Terrestrial and Aquatic Ecosystems in the Black-Forest, Southern Germany. *Journal of Quaternary Science*, 8(3), 263–276.

Lotter, A.F. & Anderson, N.J., (2012) Limnological Responses to Enbironmental Changes at Inter-annual to Decadal Time-scales. In H. J. B. Birks et al., eds. *Tracking Environmental Change Using Lake Sediments, Developments in Paleoenvironmental Research 5*. New York, NY: Springer, pp. 557–578.

Mack, R.N., Rutter, N.W., Bryant, V.M. & Valastro, S., (1978) Late Quaternary Pollen Record from Big Meadow, Pend Oreille County, Washington. *Ecology*, 59(5), 956–965.

Mack, R.N., Rutter, N.W. & Valastro, S., (1983) Holocene vegetational history of the Kootenai River Valley, Montana. *Quaternary Research*, 20(2), 177–193.

Martin, R.S. et al., (2009) Environmental effects of ashfall in Argentina from the 2008 Chaitén volcanic eruption. *Journal of Volcanology and Geothermal Research*, 184(3-4), 462–472.

McNutt, S.. & Davis, C., (2000) Lightning associated with the 1992 eruptions of Crater Peak, Mount Spurr Volcano, Alaska. *Journal of Volcanology and Geothermal Research*, 102(1-2), 45–65.

Mehringer, P.J., Arno, S.F. & Petersen, K.L., (1977a) Postglacial History of Lost Trail Pass Bog, Bitterroot Mountains, Montana. *Arctic and Alpine Research*, 9(4), 345–368.

Mehringer, P.J., Blinman, E. & Petersen, K.L., (1977b) Pollen influx and volcanic ash. *Science (New York, N.Y.)*, 198(4314), 257–61.

Millar, C., King, J., Westfall, R., Alden, H. & Delany, D., (2006) Late Holocene forest dynamics, volcanism, and climate change at Whitewing Mountain and San Joaquin Ridge, Mono Count, Sierra Nevada, CA, USA. *Quaternary Research*, 66, 273–287.

Moore, P., Webb, J. & Collinson, M., (1991) *Pollen analysis*, Oxford: Blackwell Scientific Publications.

Mullineaux, D.R., (1974) Pumice and other pyroclastic deposits in Mount Rainier National Park, Washington. *Geological Survery Bulletin*, 1326, 1–80.

NOAA, (2014) NOAA satellite and information service. Available from: http://cdo.ncdc.noaa.gov/cgi-bin/climaps/climaps.pl [Last accessed: 14/08/2014]

Orloci, L., (1966) Geometric Models in Ecology: I. The Theory and Application of Some Ordination Methods. *Journal of Ecology*, 54(1), 193–215.

Patterson, W.A., Edwards, K.J. & Maguire, D.J., (1987) Microscopic charcoal as a fossil indicator of fire. *Quaternary Science Reviews*, 6(1), 3–23.

Payne, R. & Blackford, J., (2008) Distal volcanic impacts on peatlands: palaeoecological evidence from Alaska. *Quaternary Science Reviews*, 27(21-22), 2012–2030.

Payne, R. & Blackford, J., (2005) Simulating the impacts of distal volcanic products upon peatlands in northern Britain: an experimental study on the Moss of Achnacree, Scotland. *Journal of Archaeological Science*, 32(7), 989–1001.

Philippsen, B., (2013) The freshwater reservoir effect in radiocarbon dating. *Heritage Science*, 1(1), 1–24.

Porter, S.C., (1978) Glacier Peak tephra in the North Cascade Range, Washington: Stratigraphy, distribution, and relationship to late-glacial events. *Quaternary Research*, 10(1), 30–41.

Porter, S.C. & Swanson, T.W., (1998) Radiocarbon age constraints on rates of advance and retreat of the Puget Lobe of the Cordilleran Ice Sheet during the Last Glaciation. *Quaternary Science Reviews*, 50, 205-213.

Power, M.J., Whitlock, C. & Bartlein, P.J., (2011) Postglacial fire, vegetation, and climate history across an elevational gradient in the Northern Rocky Mountains, USA and Canada. *Quaternary Science Reviews*, 30(19-20), 2520–2533.

Prentice, I., (1985) Pollen representation, source area, and basin size: toward a unified theory of pollen analysis. *Quaternary Research*, 23(1), 76–86.

Prichard, S.J., Gedalof, Z., Oswald, W.W. & Peterson, D.L., (2009) Holocene fire and vegetation dynamics in a montane forest, North Cascade Range, Washington, USA. *Quaternary Research*, 72(1), 57–67.

Pyne-O'Donnell, S.D.F. et al., (2012) High-precision ultra-distal Holocene tephrochronology in North America. *Quaternary Science Reviews*, 52, 6–11.

Rao, C., (1964) The use and interpretation of principal component analysis in applied research. *Sankhyā: The Indian Journal of Statistics, Series A*, 26(4), 329–358.

Reimer, P., (2013) IntCal13 and Marine13 Radiocarbon Age Calibration Curves 0–50,000 Years cal BP. *Radiocarbon*, 55(4), 1869–1887.

Rose, W.I. & Durant, A.J., (2009) Fine ash content of explosive eruptions. *Journal of Volcanology and Geothermal Research*, 186(1-2), 32–39.

Rubin, M. & Alexander, C., (1960) U.S. Geological Survey Radiocarbon Dates V. *American Journal of Science Radiocarbon Supplement,* 2, 129–185.

Shuman, B., (2003) Controls on loss-on-ignition variation in cores from two shallow lakes in the northeastern United States. *Journal of Paleolimnology*, 30(4), 371–385.

Staff, R.A. et al., (2011) New 14C Determinations from Lake Suigetsu, Japan: 12,000 to 0 cal BP. *Radiocarbon*, 53(3), 511–528.

Tabor, R.W., Frizzell, J.V.A., Booth, D.B., Waitt, R.B., Whetten, J.T. & Zartman, R.E., (1963) Geologic Map of the Skykomish River 30- By 60 Minute Quadrangle, Washington. *U.S. Department of the Interior*, *U.S. Geological Survery*, 1–67.

Telford, R., Barker, P., Metcalfe, S. & Newton, A., (2004) Lacustrine responses to tephra deposition: examples from Mexico. *Quaternary Science Reviews*, 23(23-24), 2337–2353.

Tesky, J.L., (1992a) Thuja plicata. In: Fire Effects Information System, [Online]. U.S. Department of Agriculture, Forest Service, Rocky Mountain Research Station, Fire Sciences Laboratory (Producer). Available from: http://www.fs.fed.us/database/feis/ [Last accessed: 24/10/2015]

Tesky, J.L., (1992b) Tsuga heterophylla. In: Fire Effects Information System, [Online]. U.S. Department of Agriculture, Forest Service, Rocky Mountain Research Station, Fire Sciences Laboratory (Producer). Available from: http://www.fs.fed.us/database/feis/plants/tree/tsuhet/all.html [Last accessed: 24/10/2015]

Thorarinsson, S., (1979) On the damage caused by volcanic eruptions with special reference to tephra and gases. In P. Sheets & D. Grayson, eds. *Volcanic Activity and Human Ecology*. New York, NY: Academic Press Inc.

Uchytil, R.J., (1989) Alnus viridis subsp. sinuata. In: Fire Effects Information System, [Online]. U.S. Department of Agriculture, Forest Service, Rocky Mountain Research Station, Fire Sciences Laboratory (Producer). Available from:

http://www.fs.fed.us/database/feis/plants/shrub/alnvirs/all.html [Last acessed: 24/10/2015]

Ugolini, F. & Dahlgren, R., (2002) Soil development in volcanic ash. *Global Environmental Research*, 6, 69–81.

Vereş, D., (2002) A Comparative Study Between Loss on Ignition and Total Carbon Analysis on Mineralogenic Sediments. *Studia UBB, Geologia*, 47(1), 171–182.

Walsh, M.K., Whitlock, C. & Bartlein, P.J., (2008) A 14,300-year-long record of fire–vegetation–climate linkages at Battle Ground Lake, southwestern Washington. *Quaternary Research*, 70(2), 251–264.

Whitlock, C., (1992) Vegetational and climatic history of the Pacific Northwest during the last 20,000 years: Implications for understanding present-day biodiversity. *The Northwest Environmental Journal*, 8, 5–28.

Wood, C. & Baldridge, S., (1990) Volcano tectonics of the Western United States. In A. Wood, Charles & J. Kienle, eds. *Volcanoes of North America, United States and Canada*. Cambridge: Cambridge University Press.

Zdanowicz, C.M., Zielinski, G.A. & Germani, M.S., (1999) Mount Mazama eruption: Calendrical age verified and atmospheric impact assessed. *Geology*, 27(7), 621–624.

Zobel, D.B. & Antos, J.A., (1997) A Decade of Recovery of Understory Vegetation Buried by Volcanic Tephra from Mount St. Helens. *Ecological Monographs*, 67(3), 317–344.